AD-A161 918 NOVEL METHODS OF DIGITAL PHASE SHIFTING TO ACHIEVE ARBITRARY VALUES OF TIME DELAY(U) DEFENCE RESEARCH ESTABLISHMENT ATLANTIC DARTMOUTH (NOVA SCOTIA) 1/1

UNCLASSIFIED A MOHAMMED SEP 85 DREA-85/106 F/G 9/5 NL

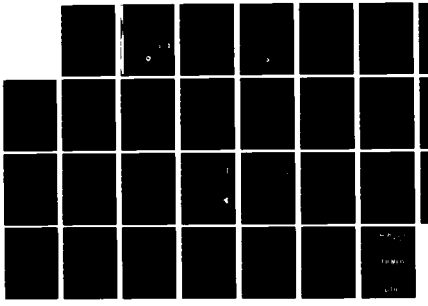

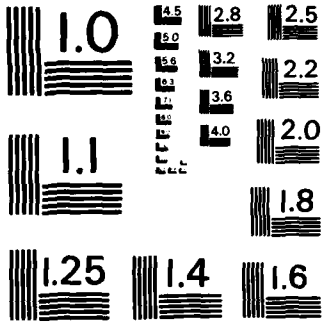

UNLIMITED DISTRIBUTION

National Defence
Research and Development Branch

Défense Nationale
Bureau de Recherche et Développment

REPORT 85/106
September 1985

NOVEL METHODS OF DIGITAL PHASE SHIFTING TO ACHIEVE ARBITRARY VALUES OF TIME DELAY

A. Mohammed

Defence Research Establishment Atlantic

Centre de Recherches pour la Défense Atlantique

Canada

DEFENCE RESEARCH ESTABLISHMENT ATLANTIC

9 GROVE STREET
P.O. BOX 1012
DARTMOUTH, N.S.
B2Y 3Z7

TELEPHONE
(902) 426-3100

CENTRE DE RECHERCHES POUR LA DÉFENSE ATLANTIQUE

9 GROVE STREET
C.P. 1012
DARTMOUTH, N.É.
B2Y 3Z7

UNLIMITED DISTRIBUTION

National Defence
Research and Development Branch

Défense Nationale
Bureau de Recherche et Développment

NOVEL METHODS OF DIGITAL PHASE SHIFTING TO ACHIEVE ARBITRARY VALUES OF TIME DELAY

A. Mohammed

September 1985

Approved by R.F. Brown Director/Underwater Acoustics Division

DISTRIBUTION APPROVED BY

CHIEF D.R.E.A.

REPORT 85/106

Defence Research Establishment Atlantic

Centre de Recherches pour la Défense Atlantique

Canada

ABSTRACT

In many signal processing applications such as in underwater acoustic array beamforming, the need arises to implement digital phase shifters. Conventional methods of implementation make use of digital interpolation and decimation to derive FIR(Finite-duration Impulse Response) realizations. Such filters, however, are capable of providing delays that are only rational fractions of the unit delay. To obtain delays that are arbitrary factors of the unit delay, two novel methods are presented: the first method makes use of a windowing technique and the second method makes use of a frequency-sampling approach. In both methods the constraint of exactly linear phase is relaxed and the departures from linear phase are kept very small. To ensure that the new phase shifters attain a high level of performance, comprehensive error measures have been developed and applied; these performance measures consist of a normalized rms error, the phase delay error and the group delay error. Moreover, these error measures are applicable to any method of designing digital phase shifters. In addition, for the frequency-sampling designs, the concept of an effective filter length is introduced; this concept takes into account the wraparound error that arises in fast-convolution signal processing operations. Aside from the presentation of the design procedures and error measures, examples are included to illustrate the salient features of the two new methods.

RÉSUMÉ

Dans de nombreuses applications du traitement des signaux telles que la formation des faisceaux dans un réseau acoustique sous-marin, il faut introduire des déphaseurs numériques. Les méthodes classiques consistent à procéder à une interpolation et à une décimation numériques pour obtenir une résponse à une impulsion de durée finie (RIF). Cette filtration ne permet toutefois de produire que des retards qui sont des fractions rationnelles du retard unité. Pour obtenir des retards qui sont des fractions arbitraires du retard unité, on propose deux nouvelles méthodes: la première fait appel à une technique de fenêtrage, et la deuxième, à un échantillonnage des fréquences. Dans les deux méthodes, la contrainte de linéairité parfaite des phases est levée et les écarts de linéairité sont maintenus à des valeurs très faibles. Pour s'assurer que les nouveaux déphaseurs soient très efficaces, on a mis au point et appliqué un système sophistiqué de mesure des erreurs; ces mesures de performance portent sur une erreur efficace normalisée , l'erreur de déphasage et l'erreur de retard de groupe. En outre, ces mesures d'erreur sont applicables à toute méthode de conception de déphaseurs numériques. De plus, dans la méthode de l'échantillonnage des fréquences, on introduit le concept de plage efficace de filtrage pour tenir compte de l'erreur de renouement qui découle du traitement des signaux à convolution rapide. En complément de la présentation des procédures de conception et des mesures des erreurs, des exemples viennent illustrer les caractéristiques particulières des deux nouvelles méthodes.

Contents

1 Introduction

In many signal processing applications, the need arises to implement digital phase shifters that delay a signal in time by specified values. For example, in real-time digital array beamforming, the number of sample-and-hold amplifiers may be much less than the number of data channels to be sampled. As a result, sets of time delays are required to correct for the differences in sampling instants within a group of channels processed by a single sample-and-hold amplifier. Also, time delays are required to compensate for the acoustic propagation delays experienced by the signals arriving from non-broadside directions at the various sensors [1]. To correct for the deskewing in time for differences in sampling times within a group of data channels, time-domain implementations of digital phase shifters are appropriate. To compensate for the acoustic propagation delays, frequency-sampling designs of digital phase shifters are required for array beamforming in the frequency domain. In addition, to reduce the beamforming errors arising from the time delays and to minimize the computational load in the beamforming operation, the time delays must be made as accurately as possible and the impulse response lengths of the phase shifters must be kept as small as possible. When the required time delays are integer multiples of the time sampling interval (called the unit delay), the realization of the phase shifters is trivial. When the required time delays are non-integer multiples of the unit delay, the realization is more difficult.

One method of solving the realization problem is related directly to the digital method of interpolation. In this context, Schafer and Rabiner used a frequency-domain interpretation to show that interpolation is fundamentally a linear filtering process [2]. Moreover, they examined the relative merits of FIR (Finite-duration Impulse Response) and IIR (Infinite-duration Impulse Response) digital filters and concluded that FIR filters are preferable for interpolation. Also, they argued that linear-phase FIR filters have many attractive features and indicated how such filters may be realized to give delays that are rational fractions of the unit delay — that is, delays of m/n units where m and n are integers. Their ideal interpolation scheme requires the creation of a sequence of $n-1$ zero-valued samples between each sample of the original digital sequence and the filtering of this zero-padded sequence with an ideal lowpass filter. By delaying the output of the lowpass filter by m units at the increased sampling rate and decimating the resulting sequence by the factor n, a fixed delay of m/n units at the original sampling rate is obtained. Furthermore, the entire procedure of obtaining m/n units of delay can be realized without sampling rate increases (for interpolation) and sampling rate decreases (for decimation) [2,3]. Pridham and Mucci used the above scheme to realize their digital interpolation beamformer, which left the channel sampling rate unaltered but introduced quantization errors in the time delays with a modest increase in the computational load [4,5]. To attain sufficient accuracy for beam steering, the quantization errors in the time delays must be kept low and to reduce the computational load, the lengths of the impulse responses of the digital filters must be kept small. Therefore, in the above application as well as in many others, it is important to have methods of realizing arbitrary values of time delay precisely with digital filters having

small impulse response lengths.

For non-integer factors of the time delay, neither an FIR or an IIR filter can achieve the ideal phase shifter characteristics. The FIR filter (having all zeros) cannot produce the exact all-pass amplitude response, whereas the IIR filter (having both poles and zeros) cannot give the exact linear phase response. As a result, any required delay can only be approximated through some design procedure. For rational values of time delay, Schafer and Rabiner [2], Crochiere and Rabiner [6] and Bellanger et al. [7] have developed effective implementations of single-stage and multi-stage FIR sections. For arbitrary values of time delay, however, only Sudhakar, Agarwal and Dutta Roy [8] have presented a method based on an interpolation procedure using a Taylor series expansion around the sample value nearest the required delay. Their method represents an adequate alternative to the multi-stage lowpass filtering scheme of Crochiere and Rabiner. However, their approximation requires derivatives up to the second order which leads to further approximation problems.

In all of the above methods to realize an arbitrary value of time delay, the FIR filters are constrained to have exactly linear phase. For practical applications, however, this constraint is unnecessary. Practical requirements normally call for FIR filters having nearly allpass amplitude responses and almost linear phase responses over specified bandwidths. Small deviations from the ideal responses over the specified bandwidths are acceptable and can be realized through simple FIR filter design procedures that are logical generalizations of the standard techniques. In particular, two novel methods of achieving arbitrary values of time delay with negligible errors are presented in this paper. The first method is similar to the familiar windowing technique and is appropriate for time-domain applications [9,10]. The second method is similar to the frequency-sampling technique and is appropriate for signal processing operations carried out in the frequency domain [9]. To ensure that the filters attain a high level of performance, comprehensive error measures are introduced and applied: the performance measures consist of a normalized rms error, the phase delay error and the group delay error. Further, the concept of an effective filter length for the frequency-sampling designs is introduced to ensure that the wraparound [11] error arising in fast convolution operations [12] is kept below an acceptable threshold. Finally, to illustrate the phase shifter designs possible by the two new methods, examples are included to show the small departures from the ideal responses, the extent of the errors incurred and the achievable bandwidths.

2 Windowing Technique

2.1 The Window Method

Since the frequency response $H(e^{j\omega T})$ of any digital filter is periodic in frequency with period f_s, the sampling frequency, it can be expanded in a Fourier series thus:

$$H(e^{j\omega T}) = \sum_{n=-\infty}^{\infty} h(n)\, e^{j\omega nT} \tag{2.1}$$

where

$H(e^{j\omega T})$	=	frequency response of the digital filter,
$h(n)$	=	coefficients of the Fourier series expansion,
	=	impulse response coefficients of the digital filter,
ω	=	radian frequency, and
T	=	time sampling period,
	=	$1/f_s$, reciprocal of the sampling rate.

Also, the impulse response coefficients $h(n)$ are given by

$$h(n) = \frac{T}{2\pi} \int_{-\pi/T}^{\pi/T} H(e^{j\omega T})\, e^{j\omega nT} d\omega \quad \text{for } n = 0, \pm 1, \pm 2, \ldots . \tag{2.2}$$

The representation in Equation 2.1, however, has two major drawbacks. First, the length of the impulse response $h(n)$ is infinite. Second, the filter is unrealizable because no finite amount of delay can compensate for the infinite length of the impulse response. Hence the filter resulting from Equation 2.1 is an unrealizable IIR (Infinite-duration Impulse Response) filter.

To approximate a desired frequency response $H_d(e^{j\omega T})$ by means of an FIR (Finite-duration Impulse Response) filter, the simplest method consists of truncating the series in Equation 2.1. Such truncation, however, leads to the familiar but unacceptable Gibbs' phenomenon: large ripples in the frequency response occur at the bandedges and exceed the desired height at the bandedges by about 9%. Increasing the length of the impulse response — by keeping more terms in the Fourier series expansion — merely decreases the transition widths at the bandedges where the Gibbs' phenomenon remains unaltered but confined to a smaller frequency range.

A successful FIR filter can be produced by applying the windowing technique [9] as follows:

1. The impulse response coefficients $h_d(n)$ corresponding to the desired frequency response $H_d(e^{j\omega T})$ are first determined. In most cases of practical interest, closed form expressions for $h_d(n)$ are obtainable from Equation 2.2.

2. A suitable window (weighting) function $w(n)$ of finite duration is chosen to control the convergence of the Fourier series. In a sense, the window function determines how much of the impulse response $h_d(n)$ we can see so that the term window is descriptive and appropriate.

3. Next, the window function is placed over the center of the impulse $h_d(n)$ to produce the modified sequence

$$h(n) = h_d(n)\, w(n) \tag{2.3}$$

of finite length.

4. If the finite-length impulse response $h(n)$ in Equation 2.3 contains negative indices (that is, negative values of n), the resulting filter is non-causal. To get a realizable FIR filter, the sequence $h(n)$ is shifted to the right until the leftmost index becomes non-negative.

The frequency domain interpretation of the windowing procedure is straightforward. If $H_d(e^{j\omega T})$ and $W(e^{j\omega T})$ are respectively the frequency responses of $h_d(n)$ and $w(n)$, then the windowing operation corresponds to the convolution of $H_d(e^{j\omega T})$ with $W(e^{j\omega T})$ in the frequency domain.

In the literature, the windowing procedure has been applied to the design of lowpass, bandpass and highpass FIR digital filters with the conventional linear phase constraint [9,10]. In this case, the desired amplitude response is unity over the passbands and zero in the stopbands. Also, the choice of the window function $w(n)$ is governed by two factors: first, $w(n)$ must be kept as short as possible to minimize the computational load in the implementation of the filter; second, $w(n)$ must be chosen to keep the transition width at the bandedges as narrow as possible and the levels of the ripples in the passband and stopband as low as possible. For a fixed length of the impulse $h(n)$, the requirements of narrow transition widths and low ripple levels are conflicting. As a result, tradeoffs are made among transition width, maximum ripple level in the passband, maximum sidelobe level and the decay of the envelope of the sidelobes.

In the design of digital phase shifters, the desired amplitude response is unity and the desired phase response is linear over the frequency band of interest. As above, the length of the window function must be kept as short as possible to minimize the computational load; and the window function must be chosen to keep the deviations in the amplitude and phase responses relative to the desired ones as small as possible. Also, for a fixed length of the impulse response, the requirement of small deviations from the desired amplitude and phase responses over specified bandwidths turns out to be conflicting with that of narrow transition widths. As a result, tradeoffs will be required among the following three factors: the deviations from unit amplitude, the deviations from linear phase and the useable bandwidth which is linked to the transition width.

2.2 Design Equations for Arbitrary Delays

The frequency response of the desired (ideal) phase shifter is given by

$$H_d(e^{j\omega T}) = \begin{cases} e^{-j\omega\tau} & \text{for } -\omega_c \le \omega \le \omega_c \\ 0 & \text{otherwise,} \end{cases} \tag{2.4}$$

where τ is the required time delay. The desired phase shifter delays all frequency components in the band $-\omega_c \le \omega \le \omega_c$ by τ seconds and rejects all frequencies outside of this band. For full band operation ω_c is equal to one half of the radian sampling frequency.

From Equation 2.2, the corresponding impulse response is

$$h_d(n) = \frac{\sin[2\pi F_c(n-d)]}{\pi(n-d)} \qquad \text{for } -\infty \le n \le \infty \tag{2.5}$$

where

$$\begin{aligned} F_c = \ f_cT = \ f_c/f_s = \ & \text{normalized cutoff frequency,} \\ d = \ \tau/T = \ & \text{normalized time delay.} \end{aligned}$$

Like the standard FIR designs, the impulse response in Equation 2.5 must be windowed and shifted to obtain a causal filter of finite length. Also, like the standard FIR designs, the impulse response in Equation 2.5 is symmetric whenever d is an integer or an integer$\pm$0.5 . However, unlike the standard FIR designs, the impulse response is asymmetric for other values of d. Therefore the resulting windowed impulse response $h(n)$ will not in general obey the symmetry or anti-symmetry property

$$h(n) = \pm h(N-1-n) \quad \text{for } 0 \le n \le N-1 \tag{2.6}$$

where N denotes the length of the impulse response which is also referred to as the filter length. This means that, in general, the phase response will not be exactly linear.

Windowing the desired impulse response $h_d(n)$ by the weighting function $w(n)$ produces noteworthy effects on the resulting frequency response. First, discontinuities in $H_d(e^{j\omega T})$ become transition bands in the resulting frequency response $H(e^{j\omega T})$. Since $H(e^{j\omega T})$ is the circular convolution of $H_d(e^{j\omega T})$ with the window's frequency response $W(e^{j\omega T})$, the width of the transition bands depends on the width of the main lobe of $W(e^{j\omega T})$. Second, the ripples in the sidelobes of $W(e^{j\omega T})$ produce ripples in the realizable frequency response $H(e^{j\omega T})$. Finally, the resulting filters are never optimal in any sense though some of the windows used in the filter design may satisfy some optimality criterion. Nevertheless, the windowing technique produces acceptable practical designs with a minimum of effort.

Complete listings of window functions can be found in the literature, particularly in Harris' paper [13]. Only the following three windows will be considered here because they will illustrate the salient features that lead to acceptable designs. The simplest window, illustrated in the top left and right boxes of Figure 2.1,is the rectangular one defined by

$$w(n) = \begin{cases} 1 & \text{for } -\dfrac{N-1}{2} \le n-d \le \dfrac{N-1}{2} \\ 0 & \text{otherwise,} \end{cases} \tag{2.7}$$

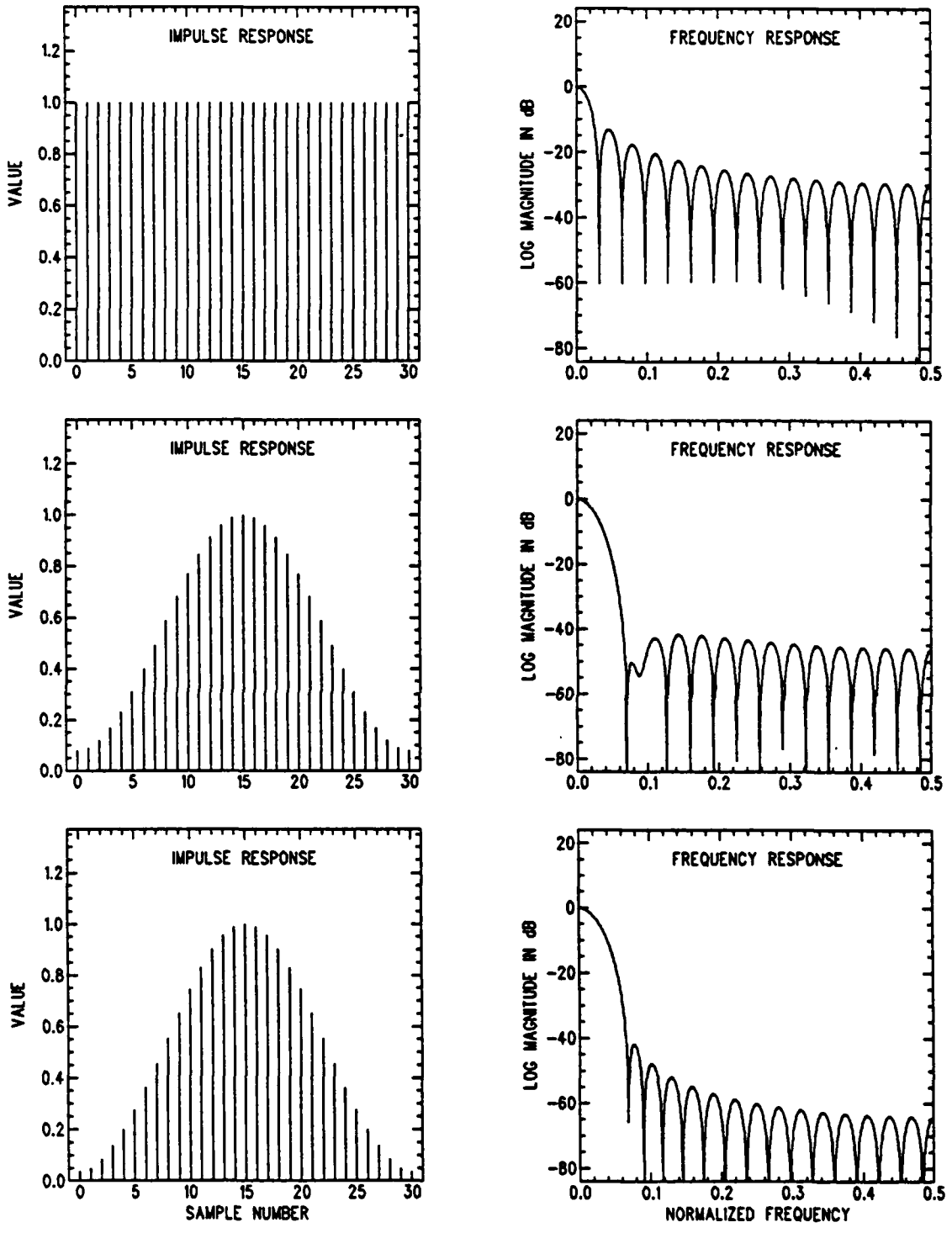

Figure 2.1: Data windows and their frequency responses: rectangular window in top two boxes; Hamming window in middle two boxes; and Kaiser window in bottom two boxes.

where n ranges from $-\infty$ to ∞. This means that the window is centered as symmetrically as possible about the middle of the window envelope – or about the peak of the envelope as in the following two windows. The rectangular window merely truncates the ideal impulse $h_d(n)$ and the corresponding frequency response exhibits the familiar Gibbs' phenomenon associated with the truncation of the Fourier series. Its frequency response $W(e^{j\omega T})$ has the smallest main lobe width of all possible windows and therefore gives the smallest transition width in digital filter designs. However, its high sidelobes produce a frequency response with a maximum stopband level (S say) of -21 dB and slowly decaying sidelobes (6 dB per octave) that are unacceptable in most applications.

By tapering the window $w(n)$ at each end, the height of the sidelobes can be reduced substantially at the expense of a wider main lobe in the frequency response of the window and thus a wider transition width in the frequency response of the digital filter. A classical example of such a window is the Hamming window illustrated in the two middle boxes of Figure 2.1 and defined by

$$w(n) = \begin{cases} 0.54 + 0.46 \cos \dfrac{2\pi(n-d)}{N-1} & \text{for} -\dfrac{N-1}{2} \le n-d \le \dfrac{N-1}{2} \\ 0 & \text{otherwise.} \end{cases} \tag{2.8}$$

The lower sidelobes of $W(e^{j\omega T})$ for this window give filter designs with a maximum stopband level of -53 dB and with sidelobes that decay very slowly.

To obtain tradeoffs between the transition width ΔF of the digital filter and its maximum stopband level S, the flexible family of windows proposed by Kaiser is recommended [10]: namely

$$w(n) = \begin{cases} \dfrac{I_0[\alpha\sqrt{1-\{2(n-d)/(N-1)\}^2}]}{I_0(\alpha)} & \text{for} -\dfrac{N-1}{2} \le n-d \le \dfrac{N-1}{2} \\ 0 & \text{otherwise,} \end{cases} \tag{2.9}$$

where

$I_0(x)$ = modified Bessel function of the 1st kind of order 0 and argument x, and

α = parameter that specifies the tradeoff between the transition width and the maximum stopband level.

The two boxes at the bottom of Figure 2.1 show the shape of this window for $\alpha = 5.658$ and its corresponding frequency response. For this value of α, the Kaiser window tapers off toward zero much more rapidly than either the rectangular or Hamming. Mathematically, of all bandlimited functions, the zero order prolate spheroidal window function provides the greatest concentration of energy in the passband and is optimum in the sense of having the maximum energy in the main lobe of $W(e^{j\omega T})$ for a given peak sidelobe level. To circumvent the difficulty of computing the prolate spheroidal function, Kaiser introduced the approximation using the I_0 function. This window with the adjustable parameter α gives the designer the flexibility to produce quick and effective FIR digital filters for signal processing applications.

For the design of digital phase shifters – and of similar digital filters – empirical values can be determined for the specifications of the following quantities:

$$\begin{array}{lcl} \Delta F = \Delta f / f_s & = & \text{normalized transition width} \\ S(\text{in dB}) & = & \text{maximum stopband ripple height} \\ P(\text{in dB}) & = & \text{maximum passband ripple height.} \end{array}$$

The transition width satisfies an equation of the form

$$\Delta F \approx C/(N-1) \tag{2.10}$$

where C is a constant depending only on the shape of the window: that is, the normalized transition width ΔF is approximately inversely proportional to the window length N. Also, as mentioned earlier, the sidelobes of $W(e^{j\omega T})$ control the height of the ripples in the passband and stopband. Moreover, in the case of the window method, the maximum ripple height $\delta_{\max}$ in the passband is equal to that in the stopband. Therefore the maximum passband ripple height in dB is given by

$$P(\text{in dB}) = \pm\, 20 \log_{10}(1 + \delta_{\max}) \tag{2.11}$$

and the maximum stopband ripple height in dB by

$$S(\text{in dB}) = 20 \log_{10}\delta_{\max}\,. \tag{2.12}$$

Table 2.1 gives the design data, derived empirically, for the amplitude characteristics of digital phase shifters based on the window method. It shows the inter-relationships among ΔF (the normalized transition width), S (the maximum stopband ripple height in dB) and P (the maximum passband ripple height in dB) for the various windows. In particular, the flexibility of the Kaiser window with its adjustable α parameter is quite evident: as α increases from 2.210 to 8.960 the maximum stopband ripple height decreases from -30 dB to -90 dB and the maximum passband ripple height decreases from 0.27 dB to 0.00027 dB as the normalized transition width increases from $1.54/(N-1)$ to $5.71/(N-1)$.

2.3 Error Measures and Design Data

To evaluate the performance of digital phase shifters, two types of errors should be considered. The first type is the mean-squared error of the phase shifter output relative to the ideal output at any instant over the useful passband for a wide-sense stationary input. This error, normalized by the mean-squared value of the input, gives a suitable measure of statistical performance. The second type of error is the time delay error. For this type, the error in the delay associated with a single frequency component defines the phase delay error, whereas the error in the delay associated with a small (infinitesimal) band of frequency components defines the group delay error. Though expressions for the above types of errors can be derived, the values of the errors have to be determined empirically to facilitate the design of the digital phase shifters.

Table 2.1: Design Data for Amplitude Response using the Window Method

Data Window	Normalized Transition Width ΔF	Maximum Stopband Ripple Height S(in dB)	Maximum Passband Ripple Height P(in dB)
Rectangular	$1.21/(N-1)$	-21	± 0.74
Hamming	$3.45/(N-1)$	-53	± 0.019
Kaiser			
α value			
2.210	$1.54/(N-1)$	-30	± 0.27
3.384	$2.23/(N-1)$	-40	± 0.086
4.538	$2.93/(N-1)$	-50	± 0.027
5.658	$3.62/(N-1)$	-60	± 0.0087
6.764	$4.32/(N-1)$	-70	± 0.0027
7.865	$5.02/(N-1)$	-80	± 0.00087
8.960	$5.71/(N-1)$	-90	± 0.00027

In Appendix A, an upper bound on the normalized rms error ϵ_{rms} is derived: namely,

$$\epsilon_{\text{rms}} \leq [\delta_{\max}^2 + |\theta - \theta_d|_{\max}^2]^{1/2} \tag{2.13}$$

where

$$\begin{aligned} \delta_{\max} &= \text{maximum deviation (ripple height) in the amplitude of the frequency response } H(e^{j\omega T}), \\ |\theta - \theta_d|_{\max} &= \text{maximum deviation in the phase of the frequency response,} \\ \theta &= \arg H(e^{j\omega T}), \\ \theta_d &= \omega\tau, \end{aligned}$$

and where these deviations are within the passband of the phase shifter. The upper bound in (2.13) is based on the premise that, in acceptable designs of digital phase shifters, both the amplitude and phase deviations from the desired (ideal) designs are small relative to unity.

The time delay errors, however, are related directly to the phase deviations $\theta - \theta_d$. In fact, the phase delay error normalized by the unit delay T is defined by

$$\Delta\tau_p = \frac{\theta - \omega\tau}{\omega T}, \tag{2.14}$$

whereas the group delay error also normalized by the unit delay T is defined by

$$\Delta\tau_g = \frac{1}{T}\frac{d(\theta - \omega\tau)}{d\omega}. \tag{2.15}$$

The quantities $\Delta\tau_p$ and $\Delta\tau_g$ give direct measures of the errors in the time delay provided by the digital phase shifter and can be evaluated numerically. In both Equations 2.14 and 2.15, θ denotes the unwrapped phase of $H(e^{j\omega T})$: that is, it refers to the continuous phase function obtained by removing the discontinuities encountered in numerical evaluation of θ by the arctan function. The method of phase unwrapping used in this paper makes use of a median filtering technique [14]. Also, to facilitate the evaluation of the phase functions and errors as well as the detailed characteristics of the phase shifters, Appendix B presents proper DFT (Discrete Fourier Transform) interpolation techniques for the purpose.

Table 2.2 gives empirical bounds on the errors ϵ_{rms}, $\Delta\tau_p$ and $\Delta\tau_g$ for the digital phase shifters designed by the window method. In this case the passband is equal to about 80% of the full bandwidth. An examination of Table 2.2 reveals the following salient features:

1. For designs in which the maximum stopband ripple height S is large (for example, the rectangular window and Kaiser window with $\alpha = 2.210$, as indicated in Table 2.1), the rms and phase errors are unacceptable.

2. Once the maximum stopband ripple height falls below about -42 dB (such as in the Hamming window and Kaiser window with $\alpha \geq 3.5$), the rms and phase errors become acceptable.

3. In the ϵ_{rms} bound, the amplitude deviations $\delta_{\max}$ in Equation 2.13 turned out to be the dominant component. In fact, for the designs using the Kaiser window, $\delta_{\max}$ accounted for about 70% of ϵ_{rms}.

Table 2.2: Error Measures for Designs using the Window Method

Data Window	Upper Bound on Normalized rms Error ϵ_{rms}	Maximum Normalized Phase Delay Error $\Delta\tau_p(\%)$	Maximum Normalized Group Delay Error $\Delta\tau_g(\%)$
Rectangular	0.090	19	34
Hamming	0.0035	2.0	4.0
Kaiser			
α value			
2.210	0.034	11	22
3.384	0.011	3.5	7.0
4.538	0.0034	1.1	2.2
5.658	0.0011	0.47	0.95
6.764	0.00034	0.15	0.30
7.865	0.00011	0.047	0.095
8.960	0.000034	0.015	0.030

NOTE: Above data apply to digital phase shifters designed by the window method and having a passband equal to 80% of the full band.

4. For time delay performance, the group delay error $\Delta\tau_g$ rather than the phase deviations $|\theta - \theta_d|$ turns out to be the most sensitive measure. As will be seen in the sample designs to be presented below, the group delay error may be unacceptable even though the phase deviations are small.

2.4 Examples

Figures 2.2-2.8 illustrate the characteristics of the digital phase shifters designed by the windowing technique. In each of these figures, the top two boxes show the impulse and frequency responses. In the impulse response diagrams (top left-hand-boxes), the sample number is actually non-negative; however, the impulse response is wrapped around the zero sample number to show the shape relative to the ideal response $h_d(n)$ in Equation 2.5. In the frequency response diagrams (top right-hand-boxes), both the amplitude and the unwrapped phase are shown; the amplitude is displayed on a dB scale and the unwrapped phase on a radian scale. The two adjoining boxes at the bottom left-hand side show the amplitude deviations ($20\ \log_{10}(1+\delta)$) and the phase deviations ($\theta - \theta_d$ in degrees) relative to the desired (ideal) phase shifter. As indicated in Equation 2.13, the amplitude and phase deviations both contribute to the normalized rms error ϵ_{rms}. Finally, the two adjoining boxes at the bottom right-hand side give the phase and group delay errors as defined in Equations 2.14 and 2.15 but on a percentage scale.

The salient features enumerated at the end of the last subsection will now be examined in greater detail. Figure 2.2 shows the unacceptably large errors for the phase shifter using the rectangular window. The errors here are smaller than those in Table 2.2 for two reasons: first, the passband is about 70% instead of 80% of the full bandwidth; and second, the normalized delay d is close to but not exactly equal to an integer$\pm$0.25 for which the impulse response has the greatest asymmetry and gives the largest phase errors.

By depressing the stopband attenuation below -40 dB, as in Figures 2.3 to 2.7 inclusively, the errors decrease dramatically by at least an order of magnitude. In Figure 2.3, the Hamming window is used, the filter length N is 31, the normalized delay d is 0.79 and the normalized cutoff frequency F_c is 0.35 (that is, 70% of the full band). In Figures 2.4 to 2.7, however, the filter length, normalized delay and design bandwidth are unchanged but the Kaiser window with its adjustable α parameter is used instead. In Figure 2.4, the value of $\alpha = 4.538$ gives a maximum passband ripple height of 0.027 dB, a normalized transition width of 0.097, a maximum stopband ripple height of -50 dB, an rms error of about 0.006, a maximum phase delay error of 0.3% and a maximum group delay error of 0.6%. In Figure 2.5 the value of α is increased to 5.658 which reduces the maximum stopband ripple height to -60 dB as well as the rms and delay errors but at the expense of a wider transition width of about 0.121. However, as the filter length is decreased from 31 in Figure 2.5 to 21 in Figure 2.6 without changing the values of α, d andF_c, the errors increase but remain within acceptable limits for practical applications.

In addition, the passband can be increased and the errors kept reasonably small by maintaining an attenuation of at least 40 dB at the edge of the full band. Figure 2.7 illustrates this point: the α value, filter length and time delay are identical to those in Figure 2.6 but the

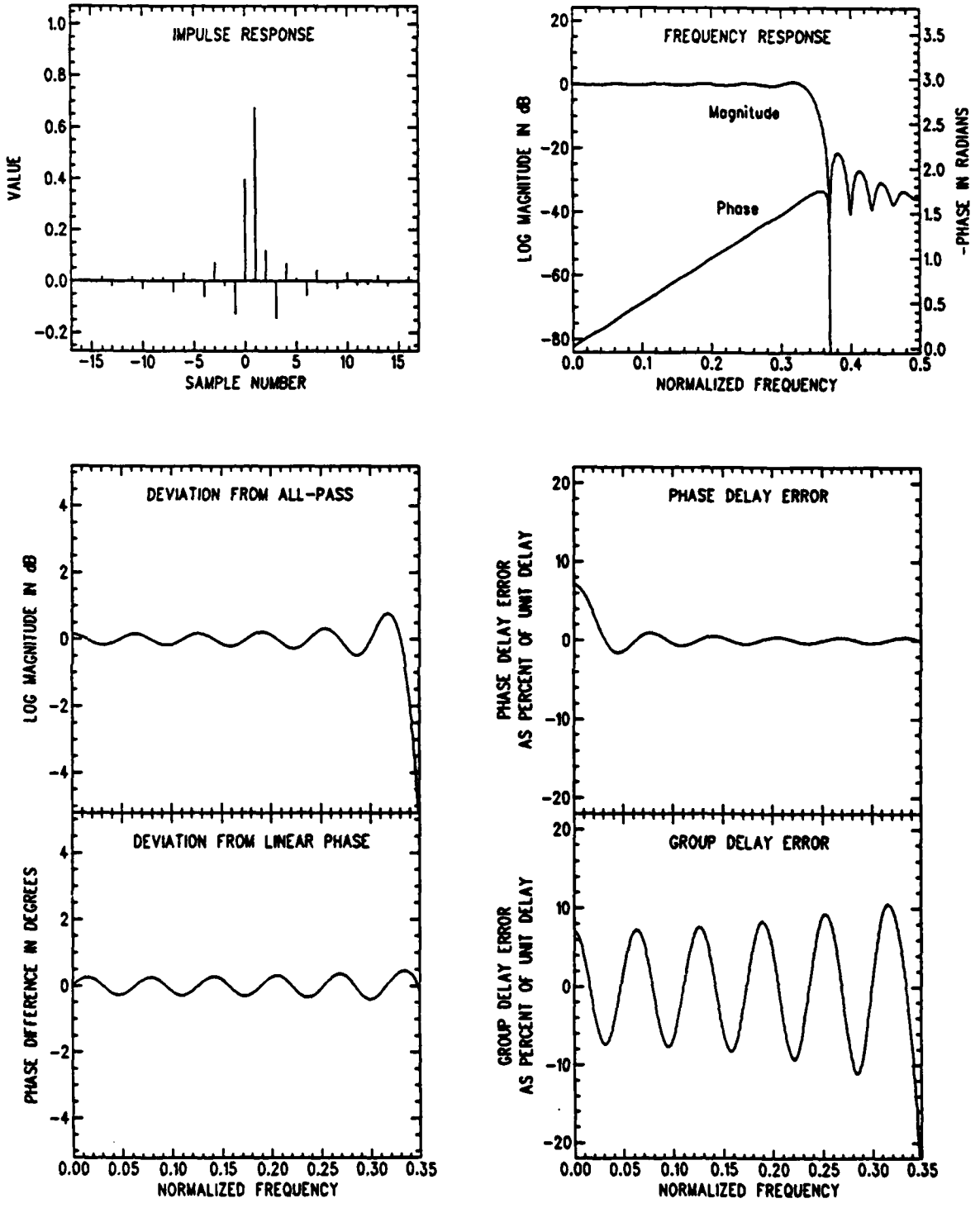

Figure 2.2: Phase shifter design using the rectangular window: $N = 31, d = 0.79, F_c = 0.35$.

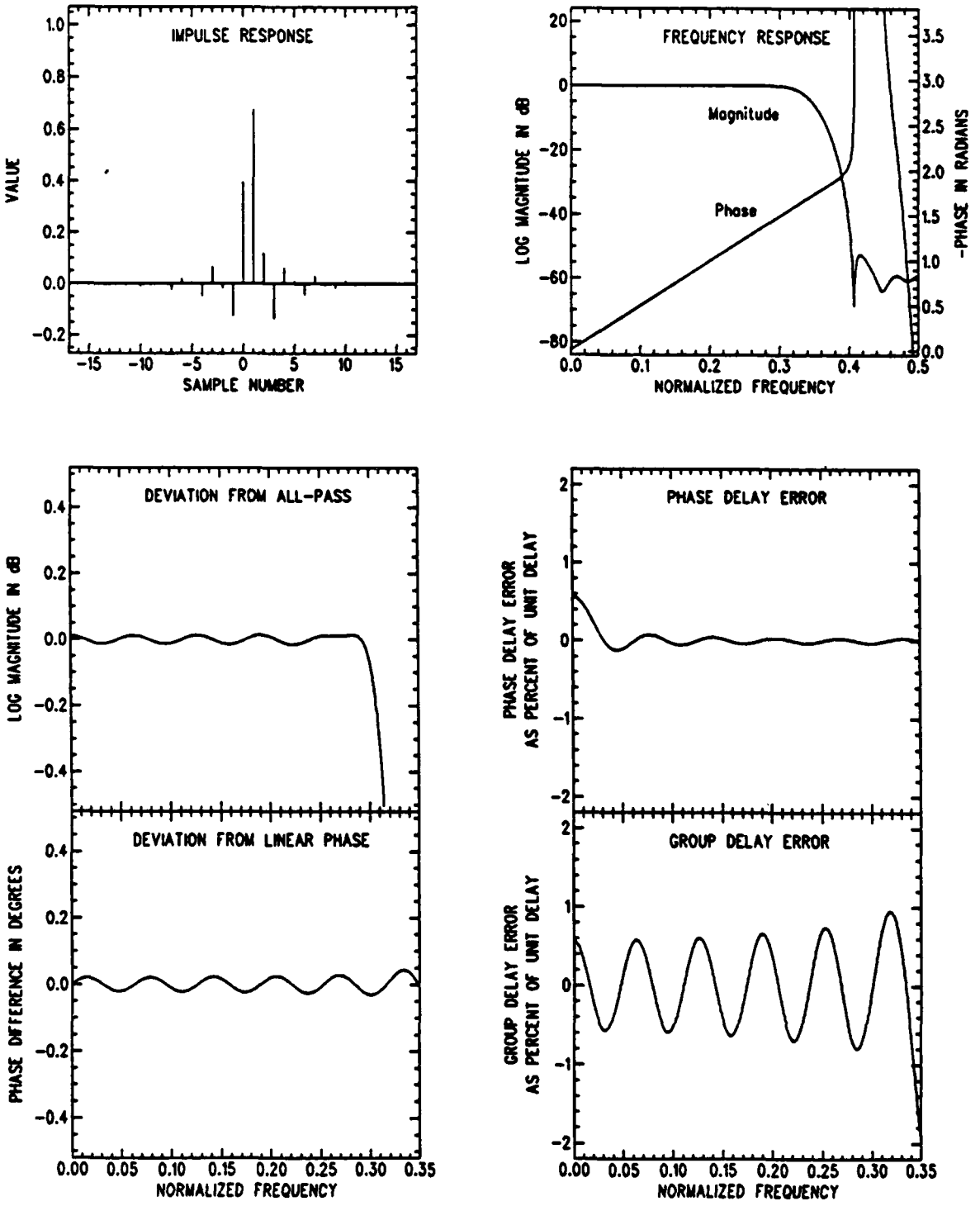

Figure 2.3: Phase shifter design using the Hamming window: $N = 31, d = 0.79, F_c = 0.35$.

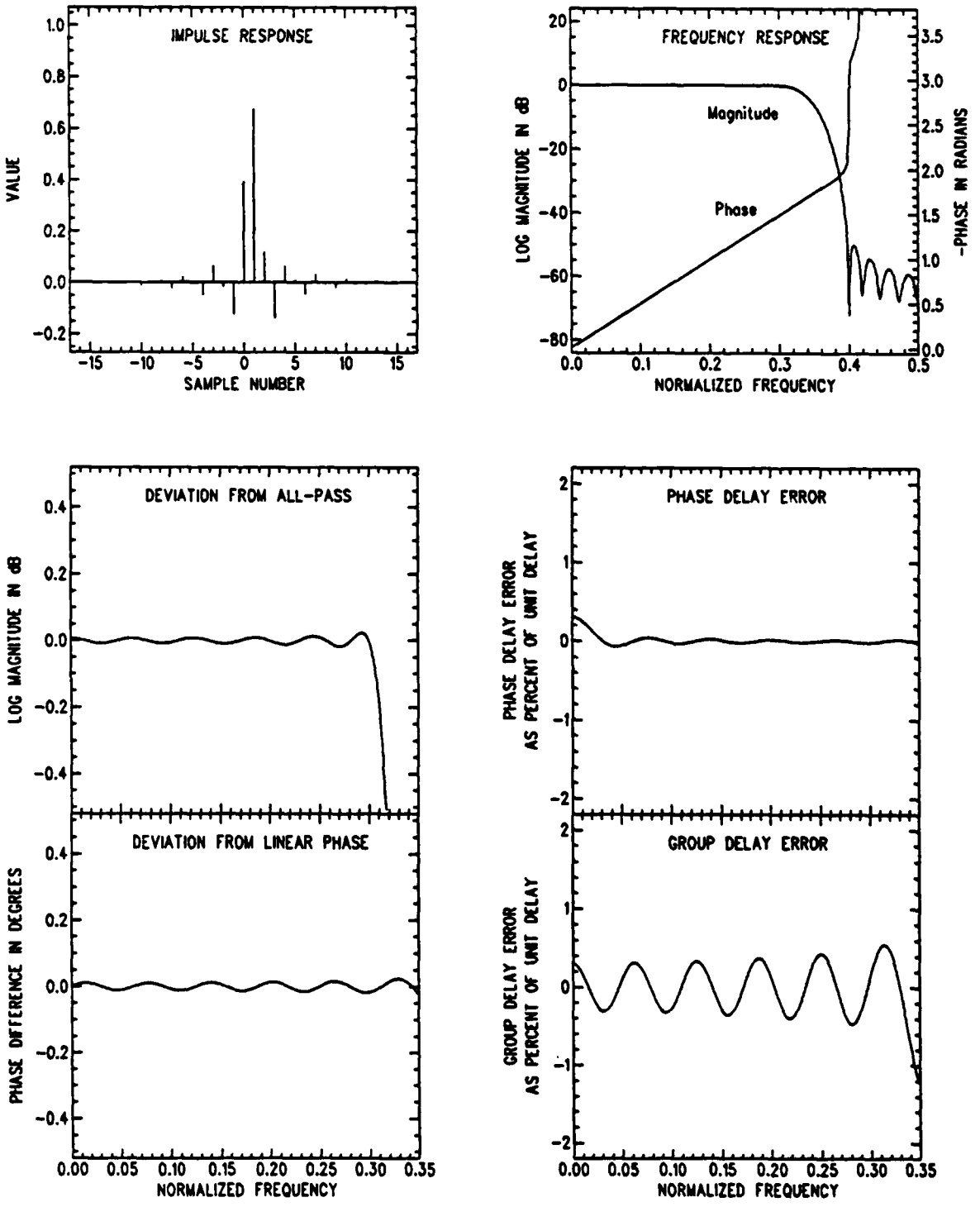

Figure 2.4: Phase shifter design using the Kaiser window: $\alpha = 4.538, N = 31, d = 0.79, F_c = 0.35$.

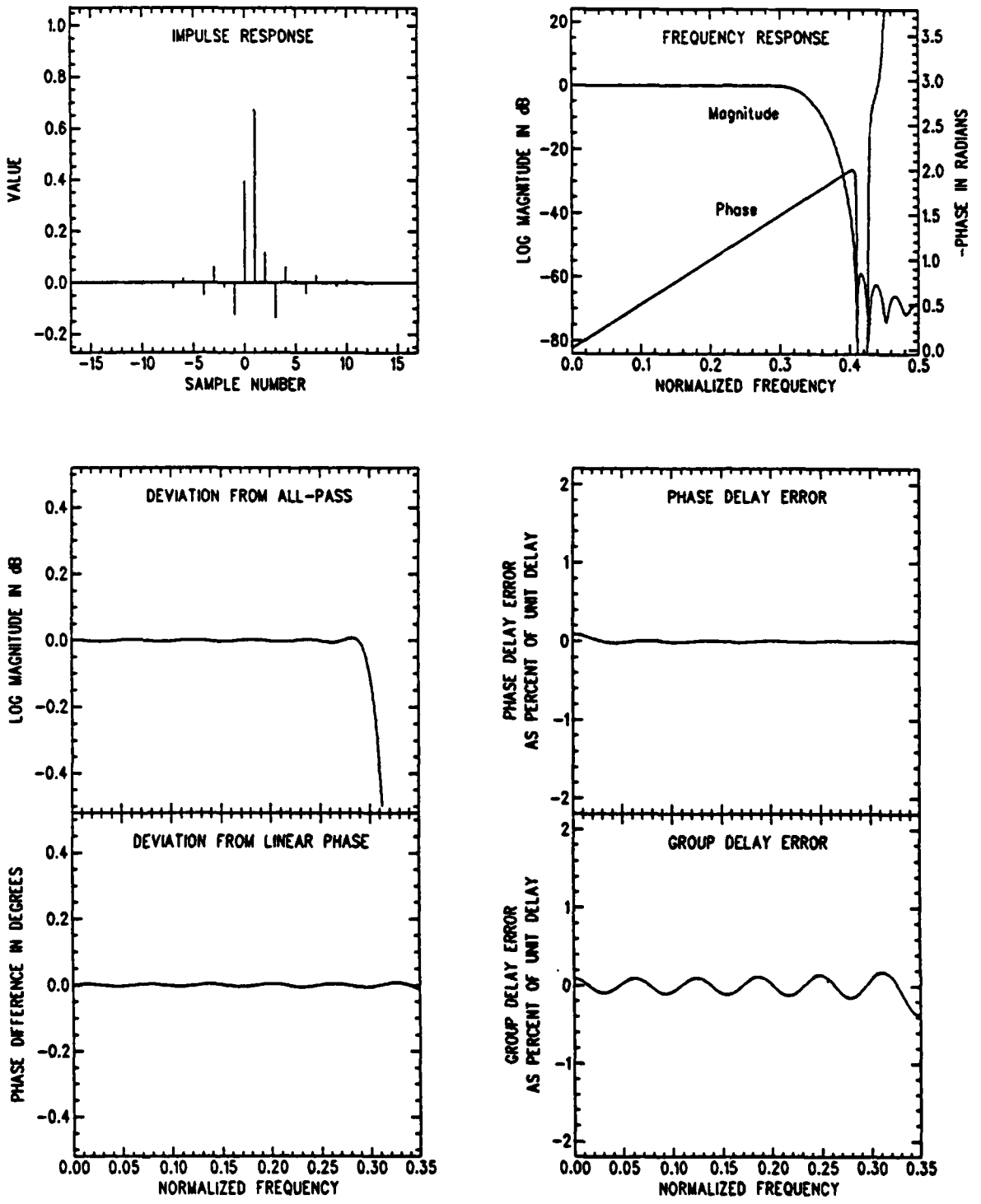

Figure 2.5: Phase shifter design using the Kaiser window: $\alpha = 5.658$, $N = 31$, $d = 0.79$, $F_c = 0.35$.

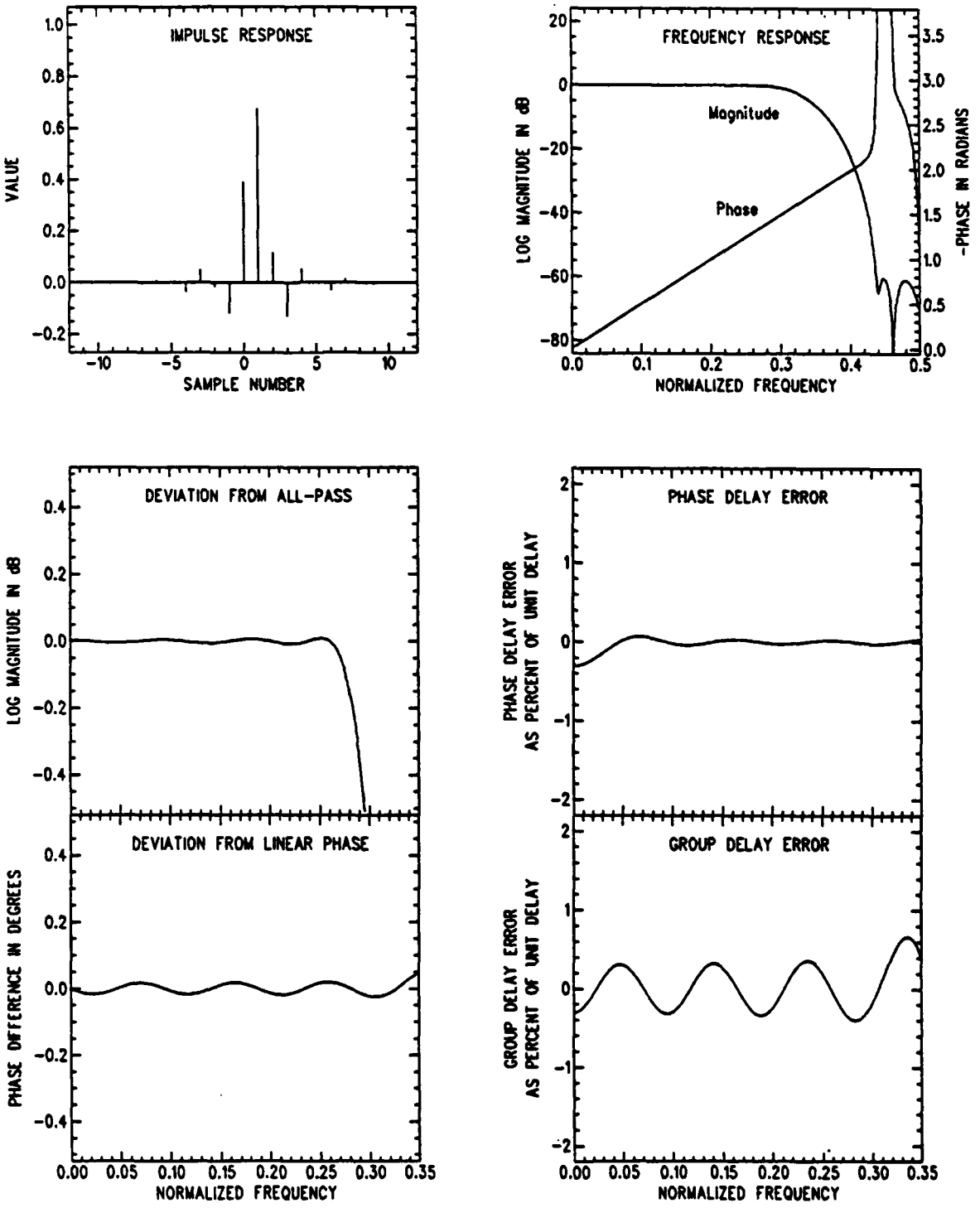

Figure 2.6: Phase shifter design using the Kaiser window: $\alpha = 5.658, N = 21, d = 0.79, F_c = 0.35$.

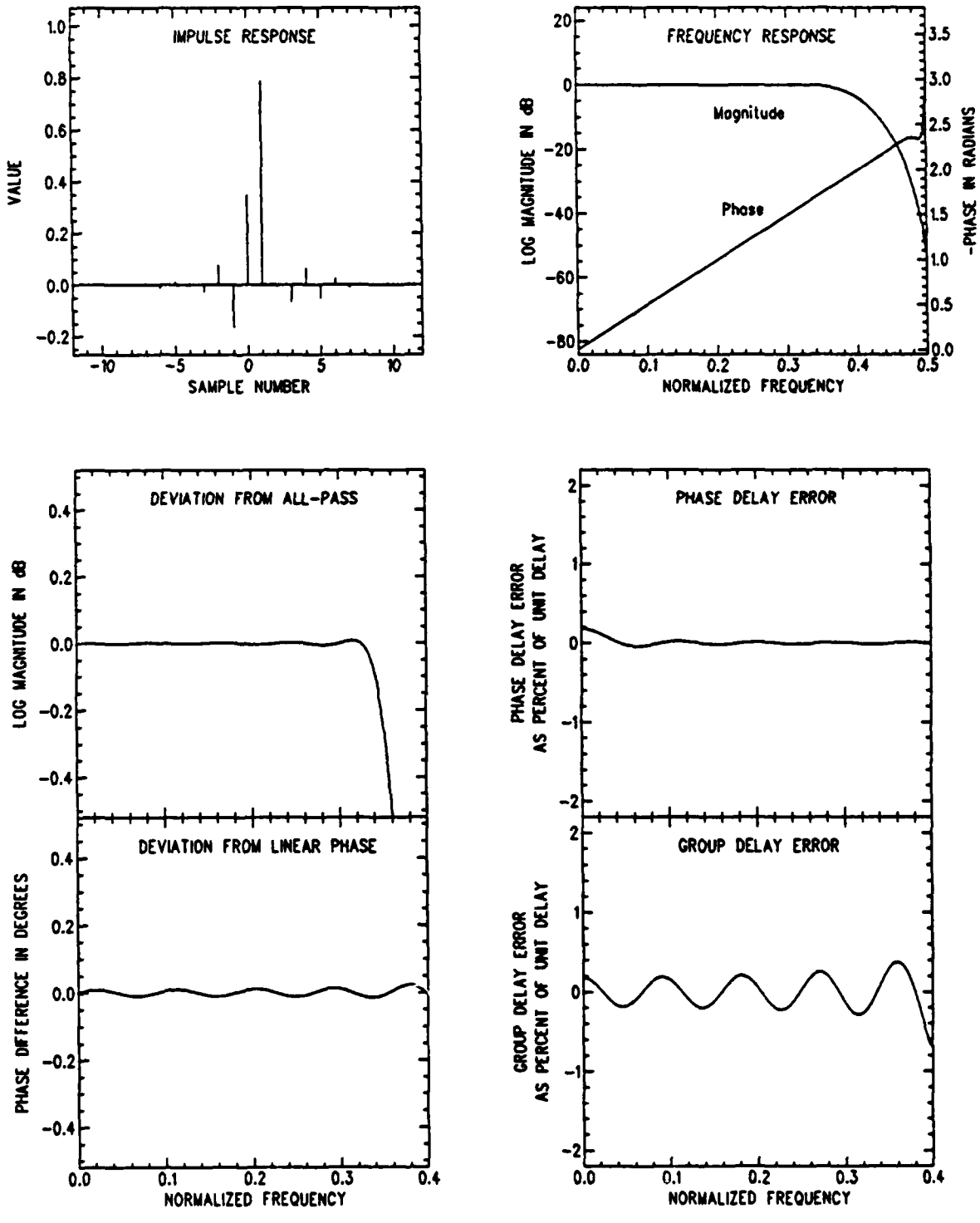

Figure 2.7: Phase shifter design using the Kaiser window: $\alpha = 5.658$, $N = 21$, $d = 0.79$, $F_c = 0.415$.

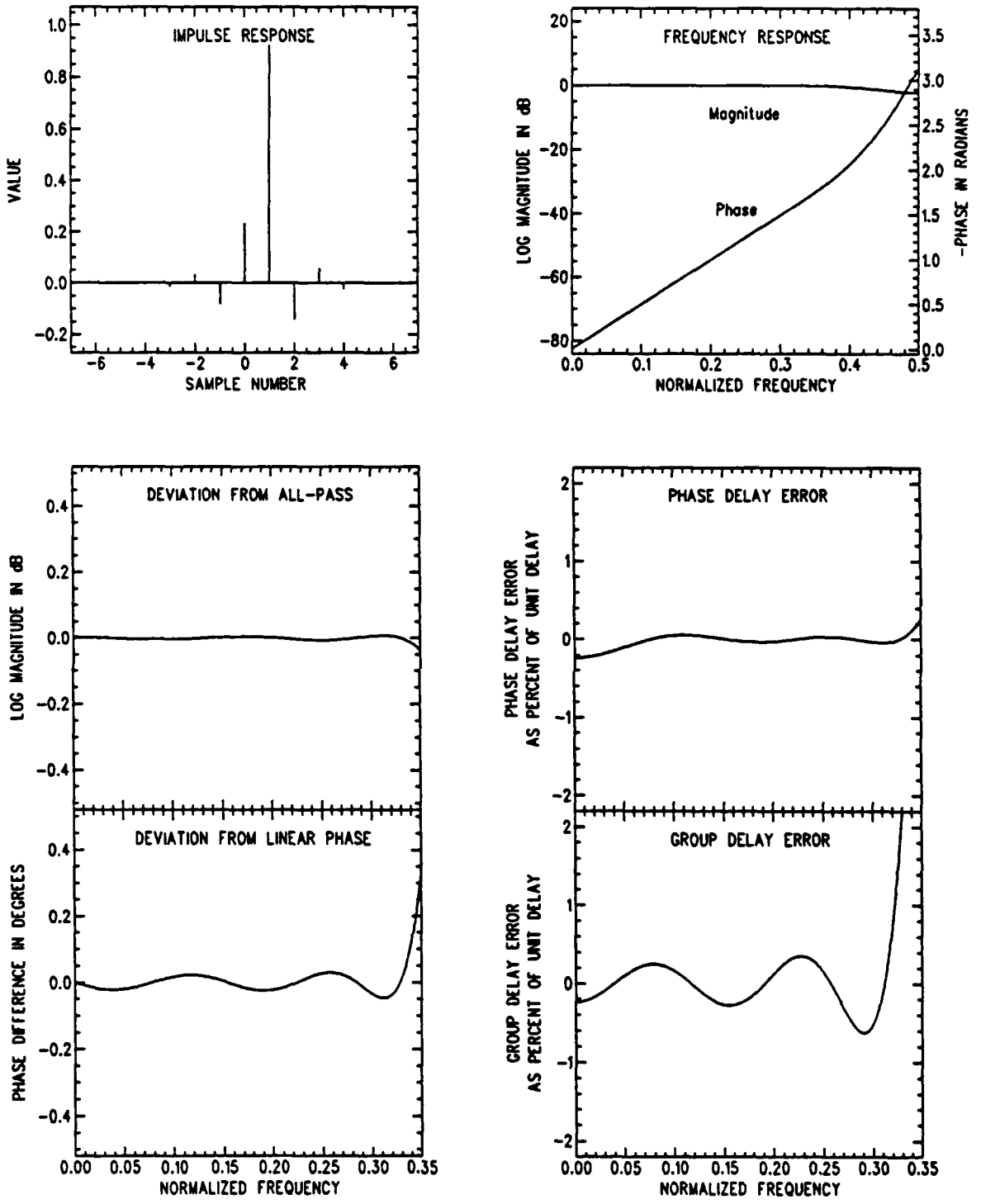

Figure 2.8: Phase shifter design using the Kaiser window: $\alpha = 5.658, N = 11, d = 0.79, F_c = 0.50$.

useful bandwidth has been extended from 70% to 80% of the full band.

To obtain acceptable designs, the following fact is important: sufficiently large attenuation (exceeding 40 dB) in the stopband translates into small phase errors (less than 1%) in the passband. This fact stems from the Hilbert transform relationships that link and restrain the amplitude and phase characteristics [15,16]. Also, any high-frequency attenuation translates into a linear phase shift at the low frequencies. In other words, without some high-frequency attenuation a linear phase shift at low frequencies would be impossible. This point is illustrated in the earlier Figures and again in Figure 2.8 corresponding to a Kaiser window with $\alpha = 5.658$ for a phase shifter of length 11 with a delay d of 0.79 and the cutoff frequency F_c pushed to the upper limit of 0.5. In the last example, the small attenuation at the high frequencies yields an almost linear phase over the band from 0 to 0.32 but produces serious phase distortions between 0.32 and 0.5. Such a design may still be useable if the band from 0.32 to 0.5 represents a "don't care" region that is eliminated in the pre-processing or post-processing operations.

3 Frequency-Sampling Technique

3.1 The Frequency-Sampling Method

Since a finite-duration sequence has a discrete Fourier transform representation, the impulse response $h(n)$ of an FIR filter can be expressed in terms of its frequency samples $H(k)$ thus:

$$H(k) = \sum_{n=0}^{N-1} h(n)\, e^{-j2\pi kn/N} \tag{3.1}$$

where

$$H(k) = H(z)|_{z=\exp(2\pi k/N)}$$

and z denotes the z-transform variable. Moreover, $H(z)$ may be expressed in terms of the frequency samples $H(k)$ as [9]

$$H(z) = \frac{1 - z^{-N}}{N} \sum_{k=0}^{N-1} \frac{H(k)}{1 - \exp(j2\pi k/N)z^{-1}}\,. \tag{3.2}$$

The substitution of $z = \exp(j\omega T)$ into Equation 3.2 gives the corresponding frequency response: namely,

$$H(e^{j\omega T}) = \sum_{k=0}^{N-1} H(k)\, \exp[-j\frac{N-1}{2}(\omega T - \frac{2\pi k}{N})]\, \frac{\sin\frac{N}{2}(\omega T - \frac{2\pi k}{N})}{\sin\frac{1}{2}(\omega T - \frac{2\pi k}{N})}\,. \tag{3.3}$$

Equation 3.3 suggests a simple method for the design of digital filters: namely, specify the frequency response only at the frequency samples $H(k)$ over one period (that is, for $k = 0, \ldots, N-1$). In this method, the interpolation formula on the right side of Equation 3.3 fills in the gaps between the frequency samples to give the complete frequency response.

For example, in the design of a lowpass FIR filter, the standard choice for the frequency samples is of the form

$$H(k) = \begin{cases} 1 & \text{for } k \text{ in the passband} \\ v_k & \text{for } k \text{ in the transition band} \\ 0 & \text{for } k \text{ in the stopband} \\ H(N-k-1) & \text{for a symmetric impulse response} \end{cases} \tag{3.4}$$

where the transition values are real and satisfy the relationship

$$1 \geq v_k \geq v_{k+1} \geq 0\,. \tag{3.5}$$

The number of transition samples and their values determine the passband ripple heights and the stopband sidelobe levels in the gaps between the frequency samples. To obtain filters whose frequency response changes quickly in a small transition band with small deviations from the ideal response in the passband and stopband, the transition values v_k should be chosen by an optimization algorithm [9,17]. For filters whose frequency response changes less quickly in the transition band, the v_k may be chosen according to some well behaved function such as a gaussian shape. However, in all designs with real-valued $H(k)$ satisfying Equation 3.4, the filters are constrained to have a fixed delay of $(N-1)T/2$ seconds. An arbitrary delay can be realized only by relaxing the rigid constraints in Equation 3.4.

3.2 Design Procedures for Arbitrary Delays

To design phase shifters that will delay the frequency components in the band $-f_c \le f \le f_c$ by τ seconds, attenuate the signals in and beyond the transition band about f_c and have real-valued impulse responses, the frequency samples must be chosen to be complex-valued and must satisfy the complex conjugate relationship

$$H(k) = H^*(N-k) \qquad \text{for } k = 0, 1, \ldots, N-1 \tag{3.6}$$

where the $*$ denotes complex conjugate. More specifically, if a_k and θ_k denote respectively the amplitude and phase components of $H(k)$, then the samples $H(k)$ are chosen as follows:

$$H(k) = a_k \exp(-j\theta_k) \tag{3.7}$$

with

$$a_k = \begin{cases} 1 & \text{for } k = 0, 1, \ldots, N_c - \lfloor (N_v-1)/2 \rfloor - 1 \\ v_k & \text{for } k = N_c - \lfloor (N_v-1)/2 \rfloor, \ldots, N_c + \lfloor N_v/2 \rfloor \\ a_{N-k} & \text{for } k = N - N_c - \lfloor N_v/2 \rfloor, \ldots, N-1 \\ 0 & \text{otherwise} \end{cases} \tag{3.8}$$

and

$$\theta_k = \begin{cases} 2\pi kd/N & \text{for } k = 0, 1, \ldots, \lfloor (N-1)/2 \rfloor \\ -\theta_{N-k} & \text{for } k = N - \lfloor (N-1)/2 \rfloor, \ldots, N-1 \\ 0 & \text{otherwise} \end{cases} \tag{3.9}$$

where

$\lfloor m \rfloor$ = integer part of the argument m
N_c = $\lfloor (f_c/f_s)N \rfloor$
= sample value corresponding to the cutoff frequency f_c
N_v = number of transition values, and
d = τ/T
= normalized time delay.

Also, the transition values v_k satisfy the same relationship as in Equation 3.5.

Equations 3.8 and 3.9 give the amplitude and phase samples at the frequency sampling points $k = 0, 1, \ldots, N-1$. In the gaps between the frequency sampling points, the deviations from the desired amplitude and linear phase characteristics depend upon the choice of the

transition values v_k, the sample integer N_c corresponding to the cutoff frequency f_c and the number of transition values N_v. A number of choices for these parameters will be given below as part of the examples. Furthermore, since the error measures developed earlier in subsection 2.3 are applicable to all phase shifters, the examples using the frequency-sampling technique will be presented in the same format as those using the windowing technique.

3.3 Examples and Further Error Consideration

In the simplest case where the number of transition values is equal to zero, it can be shown that the corresponding impulse response is given by

$$h(n) = \frac{1}{N} \frac{\sin[(2N_c - 1)\pi(d-n)/N]}{\sin[\pi(d-n)/N]} \quad \text{for } n = 0, 1, \ldots, N-1 \,. \tag{3.10}$$

In this case, the impulse response is symmetric whenever d is an integer or an integer$\pm$0.5 but is asymmetric otherwise. As mentioned earlier, filters with symmetric impulse responses have exactly linear phase, whereas those with asymmetric impulse responses have deviations from linear phase in the gaps between the frequency samples. Moreover, whenever d is equal to an integer$\pm$0.25, the deviations will be the greatest. Furthermore, in the simplest case described by Equation 3.10, the errors will be the worst as illustrated in Figure 3.1. In this example (with filter length $N = 256$, normalized delay $d = 10.79$, normalized cutoff frequency $F_c = 0.44$ and number of transition values $N_v = 0$), the deviations in amplitude from the all-pass characteristic are small but for the familiar Gibbs' phenomenon at the bandedge as well as the deviations from linear phase over the passband. However, the phase delay errors range from about 30% to 0% and the group delay errors from about 35% to 80%. Though the amplitude and phase deviations are small, the delay errors are not and make this design unacceptable.

A dramatic decrease occurs in the amplitude and phase deviations as well as in the phase delay and group delay errors when appropriate transition values v_k are used. For the same filter length ($N = 256$), delay ($d = 10.79$) and cutoff frequency ($F_c = 0.44$) as in Figure 3.1 but with three transition values (namely, $v_{111} = 0.6904$, $v_{112} = 0.2039$ and $v_{113} = 0.0135$), Figure 3.2 shows the dramatic decrease in the amplitude and phase deviations and in the delay errors. The transition values used here were taken from Table III of the paper by Rabiner et al. [17] that used an optimization procedure to minimize the amplitude deviations of lowpass filters designed by the frequency-sampling method. Though these transition values were derived to minimize only amplitude deviations, they appear to reduce phase errors substantially as well.

Optimization procedures for deriving transition values to minimize amplitude deviations are normally time consuming. Also, procedures for deriving transition values to minimize amplitude deviations and group delay errors are far more formidable to formulate and solve. Therefore, alternate, simple methods of deriving transition values are highly desirable.

One method resorts to the constraint between amplitude and phase when the requirement of linear phase over the passband is imposed. The literature reveals that the attendant amplitude response approximates a gaussian rolloff in the transition region [15,16]. This suggests

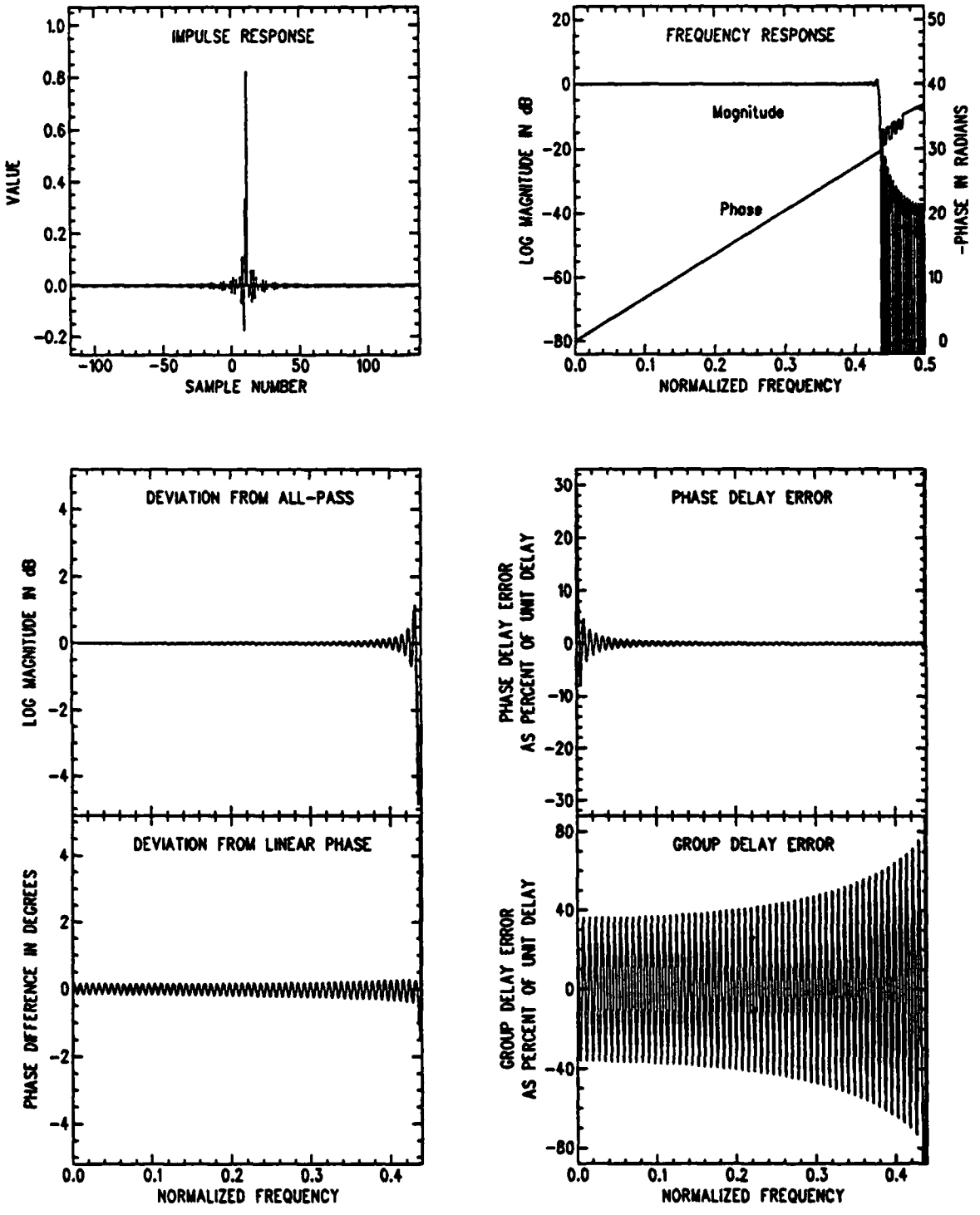

Figure 3.1: Phase shifter design using the frequency-sampling technique: $N = 256$, $d = 10.79$, $F_c = 0.44$ and $N_v = 0$ (impulse response as in Equation 3.10) .

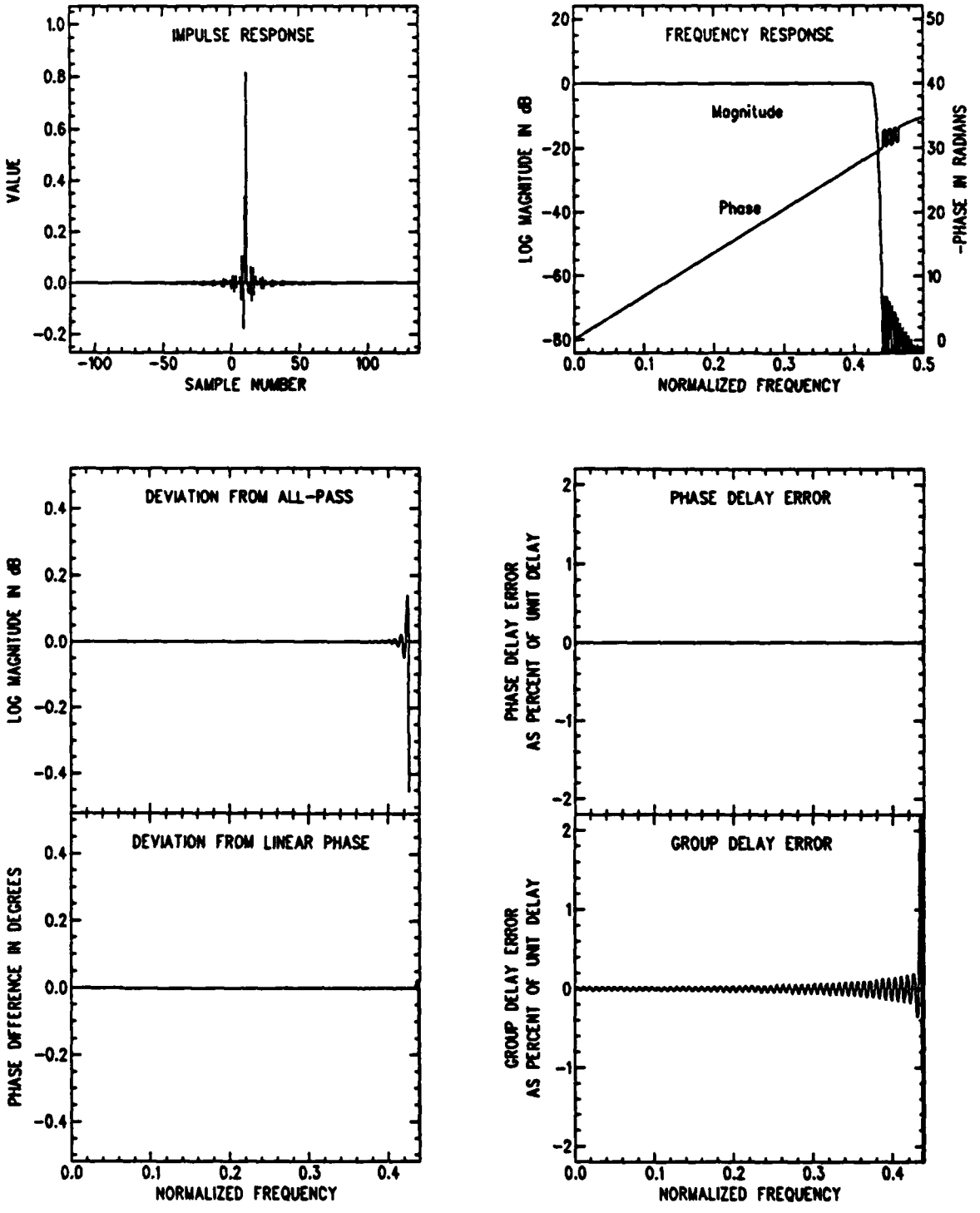

Figure 3.2: Phase shifter design using the frequency-sampling technique: $N = 256$, $d = 10.79$, $F_c = 0.44$ and three transition values $v_{111} = 0.6904$, $v_{112} = 0.2039$ and $v_{113} = 0.0135$.

that the use of a gaussian taper of the form

$$\exp(-\gamma i^2) \qquad \text{for } i = 1, 2, \ldots, N_v \tag{3.11}$$

for producing transition values should give reasonable results. For the same phase shifter design as in the last example ($N = 256$, $d = 10.79$ and $F_c = 0.44$) but for the transition values, Figures 3.3 and 3.4 show the excellent results obtainable by using seven transition values ($N_v = 7$) generated from the gaussian function in 3.11 with $\gamma = 0.15$ and 0.12 respectively.

In addition to reducing the amplitude and phase deviations and the delay errors, the use of more transition values in the frequency-sampling design gives another advantage: namely, the more gradual the amplitude rolloff in the transition region, the faster the decay of the impulse response away from its maximum value. In practical implementations, this faster decay effectively reduces the filter length. This fact becomes important in applications where frequency-sampling filters are used in fast convolution operations [12,16]. In such operations, cyclic convolutions — computed efficiently by the FFT algorithm — yield linear convolutions through the processing of overlapping data sequences; the two fast convolution procedures used in practice are referred to as the "overlap-save" and "overlap-add" methods. To avoid cyclic errors in both methods ,the amount of overlap (say M) must be at least equal to $N - 1$ (where N is the length of the impulse response). When M becomes less than $N - 1$, "wraparound" errors are introduced [11]. In fast convolution operations where the FFT length N_{FFT} is equal to the length N of the frequency-sampling phase shifter, the overlap M is less than $N - 1$ so that wraparound errors are always present. To keep the wraparound errors small, the length of the significant (essentially non-zero) portion of the impulse response (referred to as the effective filter length N_E) should not exceed the amount of overlap M.

A quantitative definition of the effective filter length N_E can be introduced through a consideration of the size of the wraparound error. In the case of the overlap-save method of fast convolution where M is less than $N - 1$, the average power spectrum of the filtered output for a stationary random input is contaminated by the wraparound error. This error corresponds to a type of aliasing that is a generalization of the aliasing produced by decimation. Quantitatively, the wraparound error is bounded by

$$\overline{E}^2 = \frac{2}{N - M} \sum_{i=1}^{N-M-1} |h(i + \lfloor d \rfloor + \lfloor M/2 \rfloor)|^2 \tag{3.12}$$

which is related directly to the mean-square error of the $N - M - 1$ tail of $h(n)$ [11]. Thus the effective filter length N_E can be defined as the smallest value of M (say $M_{\min}$) for which $\overline{E}$ remains below a specified threshold. For example,

$$N_{E,60} = M_{\min} \quad \text{for which } 20 \log_{10} \overline{E} \leq 60 \text{ dB} . \tag{3.13}$$

This definition of N_E keeps the wraparound error below a negligible level and will be used to determine the effective length of the frequency-sampling phase shifters.

For the designs in Figures 3.1, 3.2, 3.3 and 3.4, the values of $N_{E,60}$ are 256, 138, 90 and 79, respectively. In particular signal-processing applications such as frequency-domain digital beamforming [18], much smaller values of $N_{E,60}$ are required to reduce the computational load

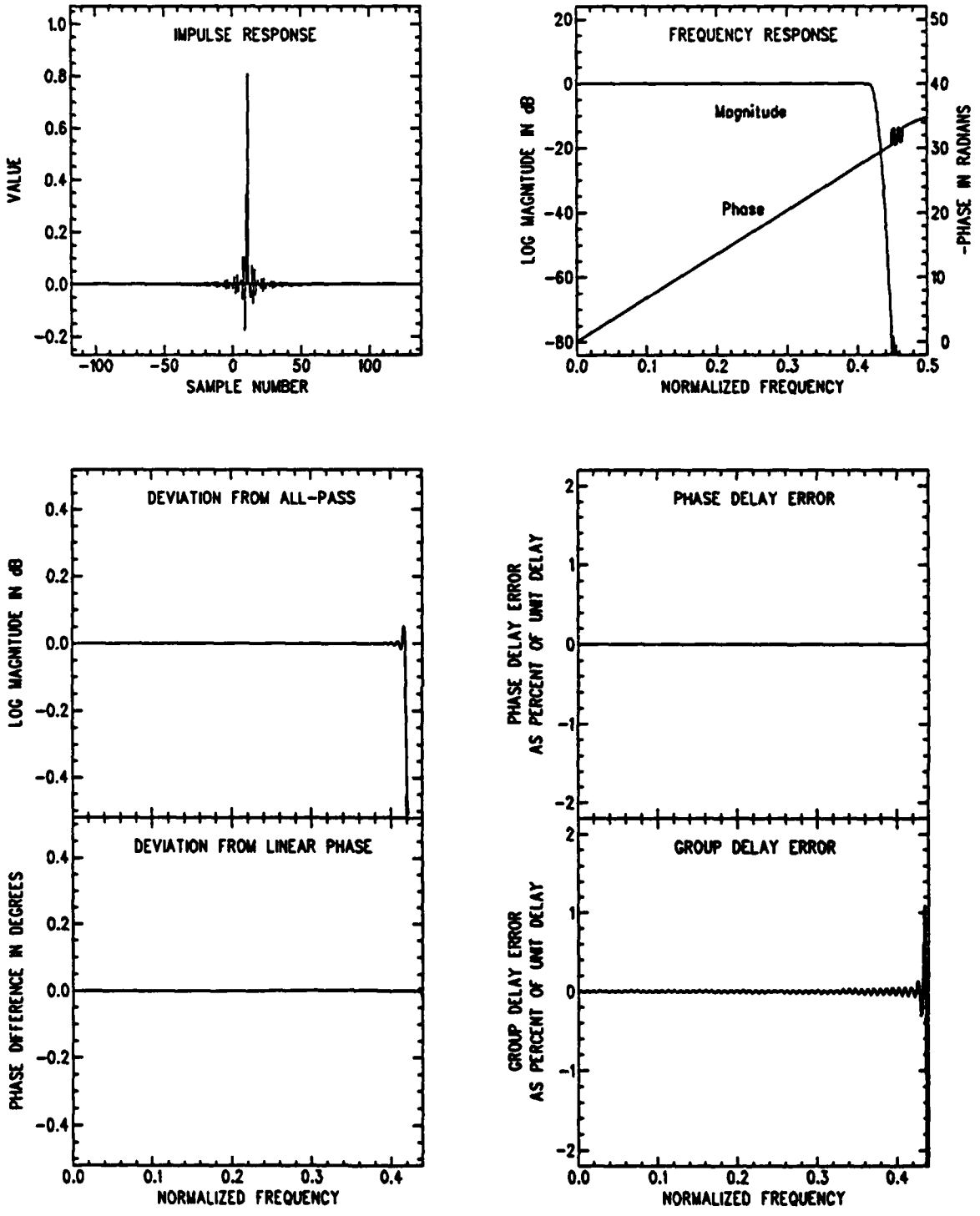

Figure 3.3: Phase shifter design using the frequency-sampling technique: $N = 256$, $d = 10.79$, $F_c = 0.44$ and seven gaussian transition values as in Equation 3.11 with $\gamma = 0.15$.

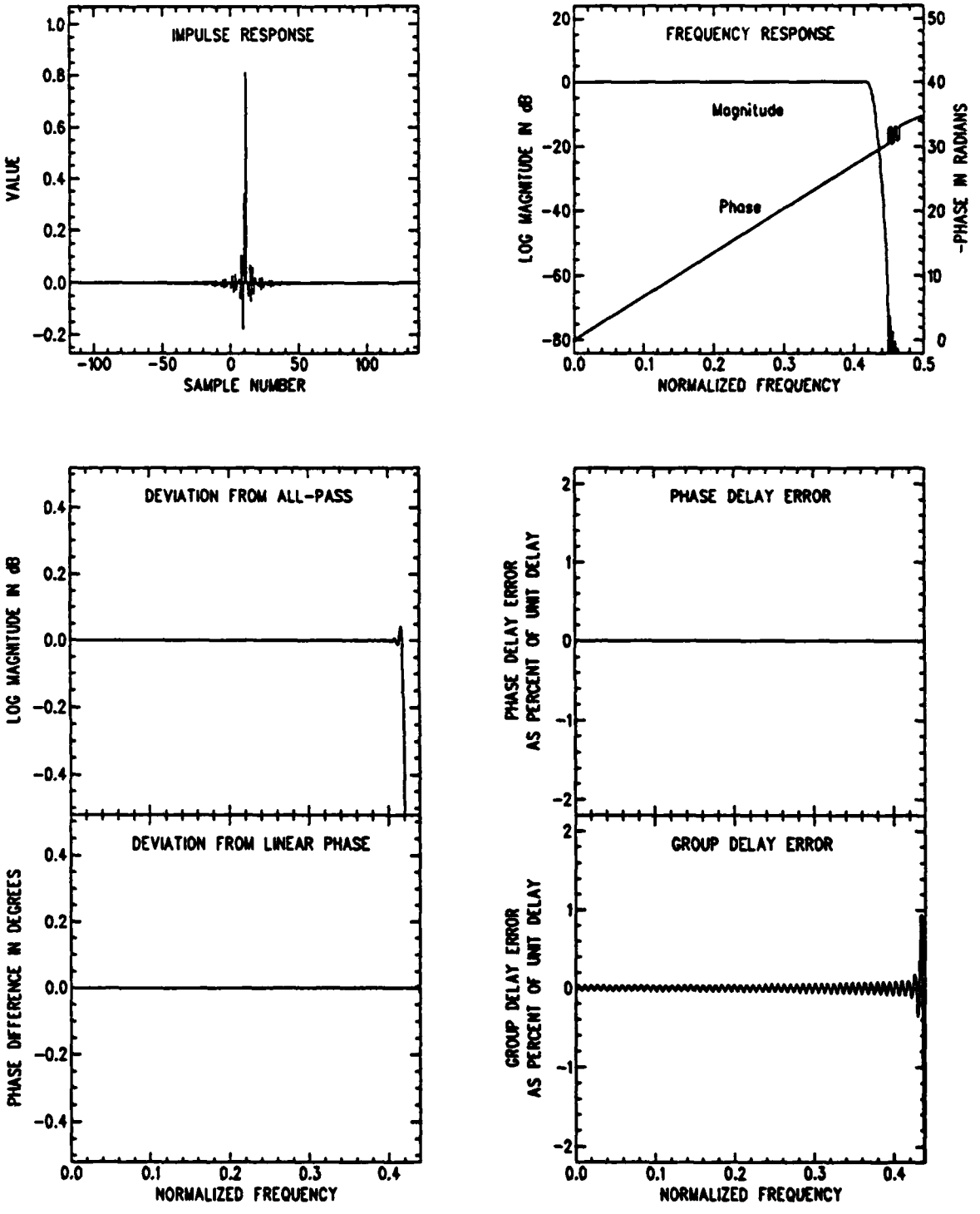

Figure 3.4: Phase shifter design using the frequency-sampling technique: $N = 256$, $d = 10.79$, $F_c = 0.44$ and seven gaussian transition values as in Equation 3.11 with $\gamma = 0.12$.

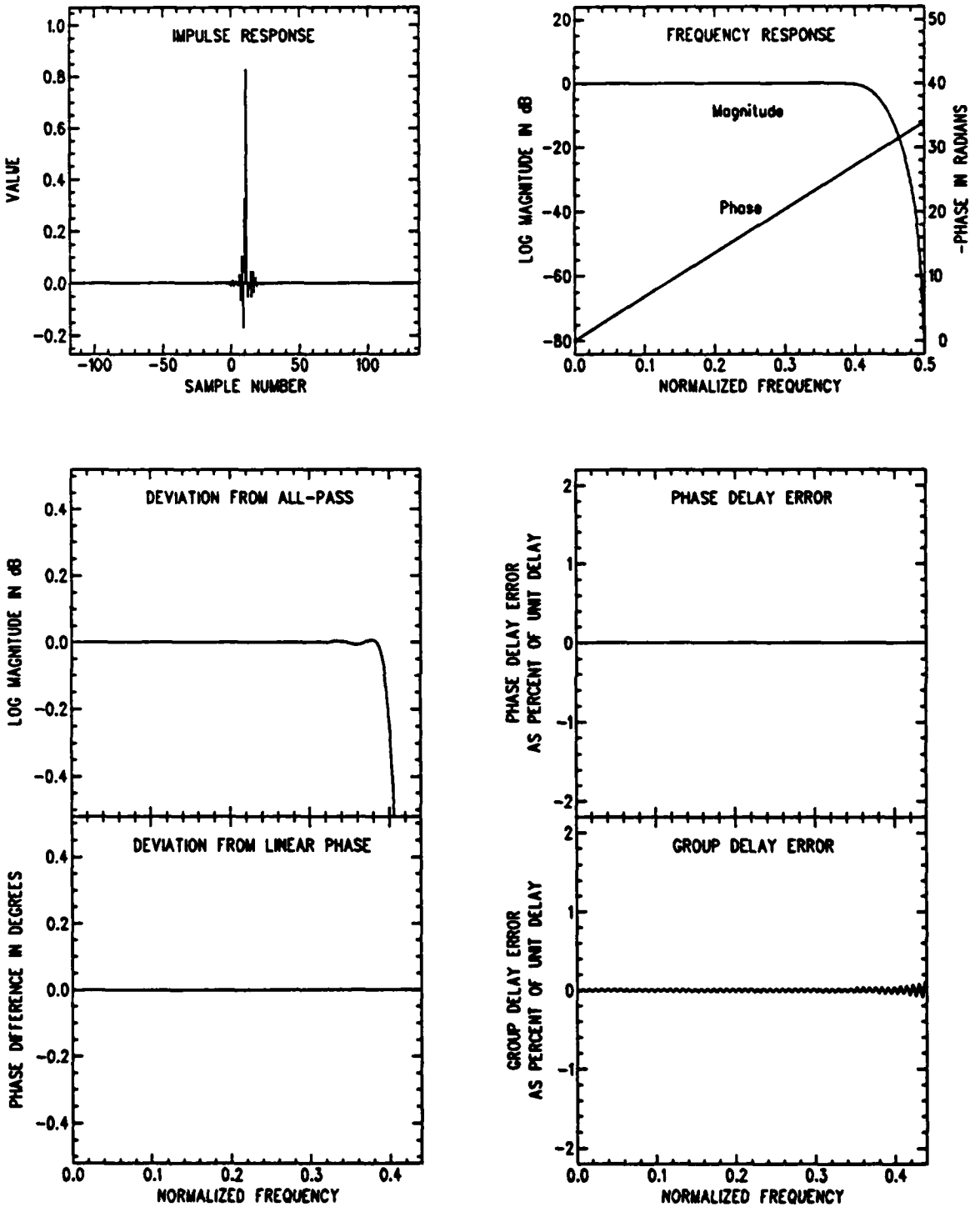

Figure 3.5: Phase shifter design using the frequency-sampling technique: $N = 256$, $d = 10.79$, $F_c = 0.44$ and transition values according to Equation 3.14 with $L = 36$ and $\gamma = 6$.

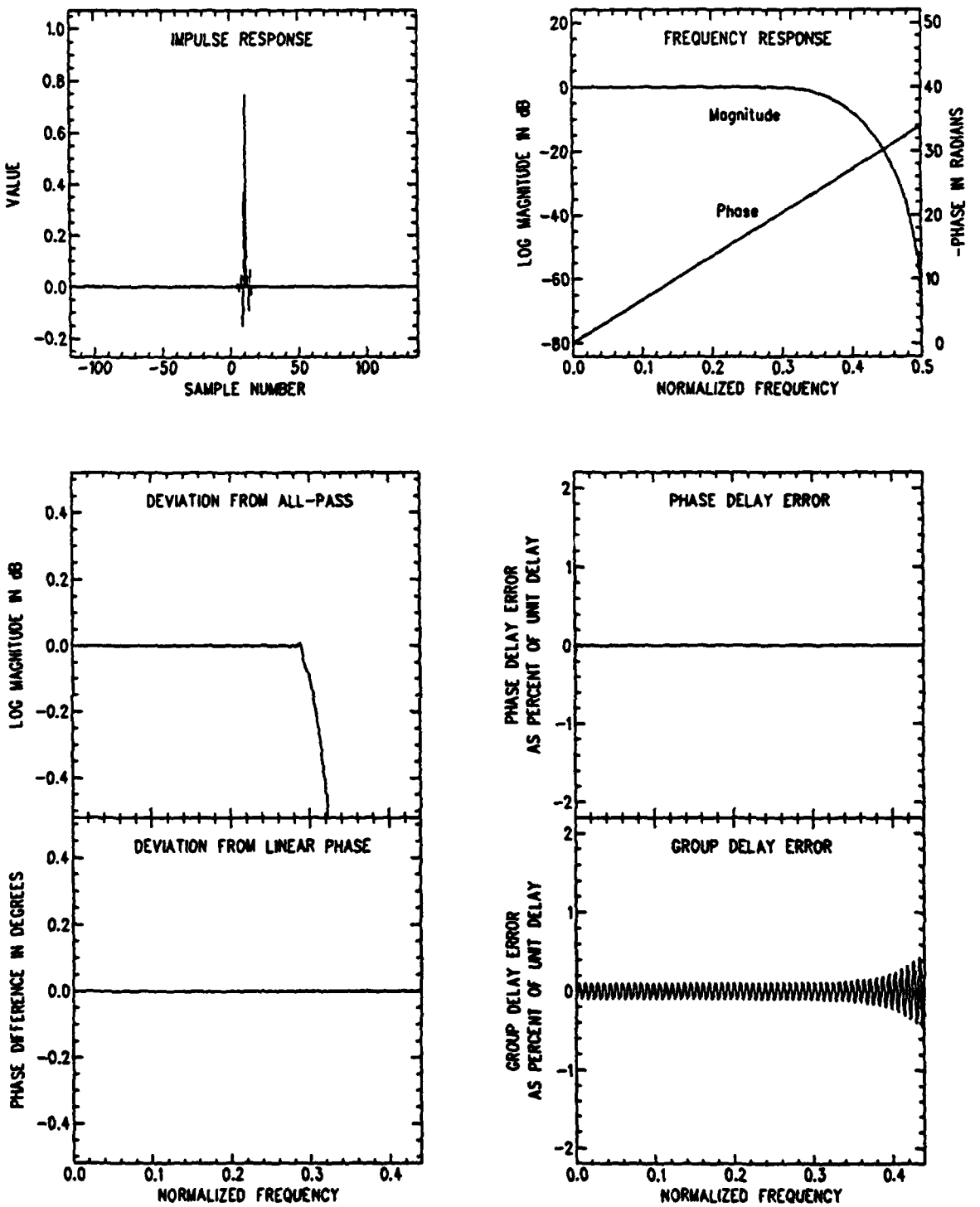

Figure 3.6: Phase shifter design using the frequency-sampling technique: $N = 256$, $d = 10.79$, $F_c = 0.39$ and transition values according to Equation 3.14 with $L = 18$ and $\gamma = 5.7$.

significantly. To design phase shifters with smaller $N_{E,60}$ values, smoother amplitude rolloffs similar to that in Figure 2.7 must be used. In fact, the transition values v_k in Equation 3.8 defining the amplitude samples of the phase shifter can be chosen from the interpolated magnitude of the frequency response of the windowed impulse response generated from Equations 2.3 and 2.5.

Figures 3.5 and 3.6 are examples of designs with effective lengths $N_{E,60}$ of 21 and 11 respectively. These designs with very small $N_{E,60}$ values were obtained by using amplitude samples a_k generated as follows:

$$a_k = \begin{cases} 1 & \text{for } k = 0, 1, \ldots, (N/4) - 1 \\ v_k & \text{for } k = (N/4), \ldots, (N/2) - 1 \quad \text{where } v_k \text{ is now the} \\ & \text{magnitude of the } N\text{-point FFT of the impulse in Eq.2.5} \\ & \text{with } d = 0.25 \text{ and weighted by the Kaiser window in Eq.2.9} \\ & \text{having length } L \ll N \text{ and adjustable parameter } \gamma \\ & \text{(with zero padding before taking FFT)} \\ a_{N-k} & \text{otherwise.} \end{cases} \tag{3.14}$$

In the case of Figure 3.5, $N = 256$, $F_c = 0.44$ and the Kaiser window is of length $L = 36$ with $\gamma = 6$; in Figure 3.6, $N = 256$, $F_c = 0.39$ and the Kaiser window is of length $L = 18$ with $\gamma = 5.7$. Other methods of generating the transition values v_k in Equation 3.14 are possible. For example, a gaussian taper could be used but would give a more or less linear rolloff on the logarithmic amplitude scale. However, the gradually increasing rolloff produced by the Kaiser window gives phase shifters with smaller effective lengths.

4 Summary

By relaxing the constraint of exactly linear phase, two novel methods of realizing digital phase shifters have been developed. Essentially, both methods are generalizations of the windowing and frequency-sampling techniques. More importantly, without the requirement of changes in the sampling rate, both methods are capable of giving arbitrary values of time delay with excellent precision. To evaluate the performance of the phase shifters, comprehensive error measures have been introduced: the performance measures include a normalized rms (root mean square) error, the phase delay error and the group delay. In addition, the concept of an effective filter length for frequency-sampling phase shifters has been introduced to keep the wraparound error arising in fast-convolution operations below acceptable thresholds.

The above methods of digital phase shifting to achieve arbitrary values of time delay as well as the set of error measures to evaluate filter performance are useful in a number of signal processing applications. For example, in real-time array beamforming for acoustic sensors, the time-domain phase shifter realizations are applicable to deskewing of time differences within a group of data channels sampled by a single sample-and-hold amplifier; and the frequency-sampling phase shifters are most appropriate in compensating for the acoustic propagation delays of signals arriving at the various sensors when beamsteering is carried out in the frequency domain. For applications such as the above, the novel and simple methods of digital phase shifting introduced in this paper are capable of producing precise time delays.

Appendix A Normalized RMS Error

Figure A.1 shows the system used to derive a statistical measure of the error of the output of the digital phase shifter. The sequence $\{y_d(n)\}$ denotes the output of the desired (ideal) phase shifter $h_d(n)$ with frequency response

$$H_d(e^{j\omega T}) = \exp[-j\theta_d(e^{j\omega T})] \tag{A.1}$$

where, from Equation 2.4,

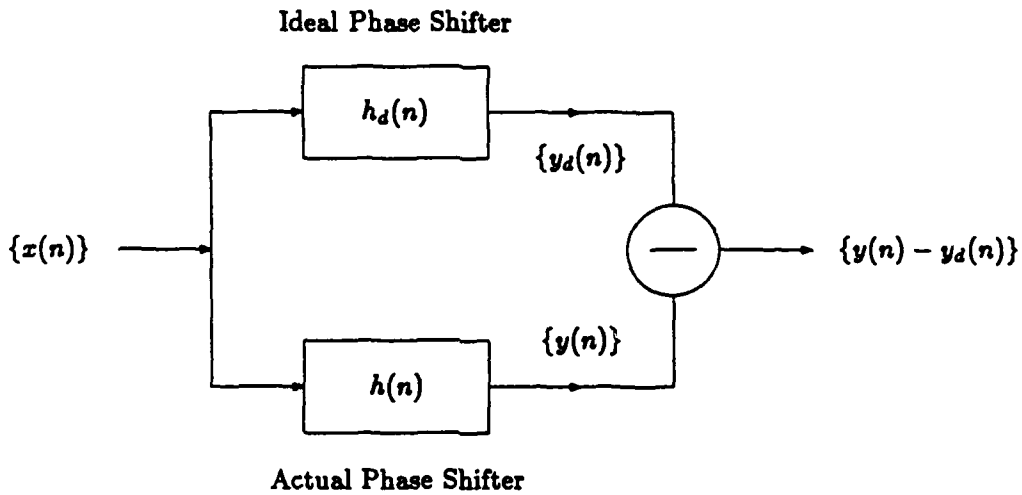

Figure A.1: System for evaluating normalized rms error.

$$\theta_d(e^{j\omega T}) = \begin{cases} \exp(-j\omega\tau) & \text{for } -\omega_c \le \omega \le \omega_c \\ 0 & \text{otherwise;} \end{cases}$$

whereas the sequence $\{y(n)\}$ denotes the output of the actual phase shifter $h(n)$ with frequency response

$$H(e^{j\omega T}) = [1 + \delta(e^{j\omega T})]\ \exp[-j\theta(e^{j\omega T})]\,. \tag{A.2}$$

In Equation A.2 $\delta(e^{j\omega T})$ represents the amplitude deviations relative to the allpass characteristic and $\theta(e^{j\omega T})$ denotes the actual phase function. Over the passband of $H(e^{j\omega T})$, the amplitude deviations would be small and the phase function $\theta(e^{j\omega T})$ would closely approximate $\theta_d(e^{j\omega T})$ for designs that are acceptable.

For a wide-sense stationary input $\{x(n)\}$, the mean square error ϵ_F^2 of the output of the actual phase shifter relative to that of the desired design over the passband $-p\pi \leq \omega T \leq p\pi$ is

$$\begin{aligned} \epsilon_F^2 &= \mathrm{E}\{[y(n) - y_d(n)]^2\} \\ &= \frac{1}{2\pi}\int_{-p\pi}^{p\pi} |H(e^{j\omega T}) - H_d(e^{j\omega T})|^2 \, |X(e^{j\omega T})|^2 \, d\omega \end{aligned} \tag{A.3}$$

where $\mathrm{E}\{u\}$ denotes the expected value of the argument u and $|X(e^{j\omega T})|^2$ is the power spectral density of $\{x(n)\}$. The error ϵ_F depends predominantly on the filter approximation error $\Delta H = |H(e^{j\omega T}) - H_d(e^{j\omega T})|$ — hence the subscript F on the ϵ. Furthermore, it can be normalized by the mean square value of $\{x(n)\}$, namely

$$E_x = E^2\{x(n)\} = \frac{1}{2\pi}\int_{-p\pi}^{p\pi} |X(e^{j\omega T})|^2 \, d\omega \, , \tag{A.4}$$

to give the normalized rms (root mean square) error

$$\epsilon_{\mathrm{rms}} = \epsilon_F / E_x \, . \tag{A.5}$$

From Equations A.1 and A.2, the filter approximation error ΔH is given by

$$\Delta H^2 = (1+\delta)^2 + 1 - 2(1+\delta)\cos(\theta_d - \theta) \, . \tag{A.6}$$

In acceptable designs both δ and $\theta_d - \theta$ are each very much less than unity. Therefore, a good upper bound for ΔH^2 and consequently of ϵ_{rms} is

$$\epsilon_{\mathrm{rms,max}} \leq [\delta_{\mathrm{max}}^2 + |\theta_d - \theta|_{\mathrm{max}}^2]^{1/2} \, . \tag{A.7}$$

This means that the maximum rms error is bounded simply by the square root of the sum of the squares of the maximum deviations in the amplitude and phase within the passband. For example, if $\delta_{\mathrm{max}} = 0.0087$ and $|\theta_d - \theta|_{\mathrm{max}} = 0.0043$, then $\epsilon_{\mathrm{rms,max}} \leq 0.0097$. Also, if $|\theta_d - \theta|_{\mathrm{max}}$ is negligible compared to δ_{max}, then $\epsilon_{\mathrm{rms,max}} \leq \delta_{\mathrm{max}}$.

Appendix B DFT Interpolation

To interpolate between DFT (Discrete Fourier Transform) coefficients, the standard procedure makes use of the familiar "zero padding" technique. This procedure is implemented as follows. If the original data sequence is

$$\{x(m)\} \quad \text{where} \quad m = 0, 1, \ldots, M-1\,, \tag{B.1}$$

then a new time series $\{y(n)\}$ is defined thus:

$$y(n) = \begin{cases} x(n) & \text{for } n = 0, 1, \ldots, M-1 \\ 0 & \text{for } n = M, \ldots, N-1 \end{cases} \tag{B.2}$$

where N is normally chosen to be a multiple of M. Next, the N-point DFT of $\{y(n)\}$ gives the interpolated DFT coefficients corresponding to the M-point DFT of $\{x(m)\}$. In fact, if

$$X(k) = \text{DFT}\ \{x(m)\} \qquad k = 0, 1, \ldots, M-1 \tag{B.3}$$

$$Y(k) = \text{DFT}\ \{y(n)\} \qquad l = 0, 1, \ldots, N-1 \tag{B.4}$$

and

$$N = rM \qquad r = \text{ integer}, \tag{B.5}$$

then

$$Y(l) = \begin{cases} X(k) & \text{for } l = rk \\ \text{interpolated values} & \text{otherwise.} \end{cases} \tag{B.6}$$

However, if the original sequence $\{x(m)\}$ has sharp edges (discontinuities) at the two ends around $m = 0$ and $m = M-1$, the standard zero padding technique would produce erroneous interpolated DFT coefficients. Since the majority of the impulse responses considered in this paper has sharp edges, a method has to be developed to give proper DFT coefficients. One method of doing so with negligible error is presented below.

Let $X(k, m_0)$ denote the DFT of $\{x((m-m_0))\}$ where $\{x((m-m_0))\}$ denotes the sequence $\{x(m)\}$ that is shifted circularly to the right by m_0 time samples. Then, in terms of $X(k) = \text{DFT}\ \{x(m)\}$,

$$X(k, m_0) = \exp(-j2\pi m_0 k/M)\ X(k)\,. \tag{B.7}$$

With this relationship, the procedure for finding interpolated DFT coefficients for a sequence $\{x(m)\}$ with sharp edges at the ends is as follows. First, the sequence $\{x(m)\}$ is shifted circularly to the right by m_0 samples so that the largest (positive and negative) values are located near the center and the smallest ones near the two ends. This circular shift produces

the sequence $\{x((m-m_0))\}$ with the DFT coefficients in Equation B.7. Second, the sequence $\{x((m-m_0))\}$ is augmented with zeros thus:

$$y(n) = \begin{cases} x((m-m_0)) & \text{for } n = 0, 1, \ldots, M-1 \\ 0 & \text{for } n = M, \ldots, N-1 \,. \end{cases} \qquad (B.8)$$

Third, the sequence $\{y(n)\}$ is shifted circularly to the right by m_1 samples, where $m_1 = N/2$, to produce the sequence

$$\{z(n)\} = \{y((n-m_1))\} \qquad n = 0, 1, \ldots, N-1 \,. \qquad (B.9)$$

This second shift places the largest values of $\{z(n)\}$ near the center of the augmented sequence. Fourth, the DFT of $\{z(n)\}$ is taken and is given by

$$\begin{aligned} Z(l) &= \exp(-j2\pi m_1 l/N)\, Y(l) \\ &= \exp[-j2\pi(m_0+m_1)l/N]\, X(l) \qquad l = 0, 1, \ldots, N-1 \,. \end{aligned} \qquad (B.10)$$

Finally, the interpolated values of the DFT of the original sequence $\{x(m)\}$ are given by

$$X(l) = \exp[j2\pi(m_0+m_1)l/N]\, Z(l) \qquad l = 0, 1, \ldots, N-1 \,. \qquad (B.11)$$

The interpolated coefficients in Equation B.11 have negligible errors and give correct amplitude and phase values.

Bibliography

[1] W.C.Knight, R.G.Pridham and S.M.Kay,"Digital Signal Processing for Sonar," *Proc. of the IEEE*, Vol.69, No.11, pp.1451–1506, Nov.1981.

[2] R.W.Schafer and L.R.Rabiner,"A Digital Signalling Processing Approach to Interpolation," *Proc. of the IEEE*, Vol.61, No.6, pp.692–702, Jun.1973.

[3] R.E.Crochiere and L.R.Rabiner,*Multirate Digital Signal Processing*, Prentice-Hall Inc., Englewoods Cliff, New Jersey, 1983, pp.271–274.

[4] R.G.Pridham and R.A.Mucci,"A Novel Approach to Digital Beamforming," *J. Acoust. Soc. Am.*, Vol.63, No.2, pp.425–434, Feb.1978.

[5] R.G.Pridham and R.A.Mucci,"Digital Interpolation Beamforming for Low-pass and Bandpass Signals," *Proc. of the IEEE*, Vol.67, No.6, pp.904–919, Jun.1979.

[6] R.E.Crochiere and L.R.Rabiner,"Optimum FIR Digital Filter Implementation for Decimation, Interpolation and Narrowband Filtering," *IEEE Trans. on Acoustics, Speech and Signal Processing*, Vol.ASSP–23, pp.444–456, Oct.1975.

[7] M.G.Bellanger, J.L.Daguet and G.P.Lapgnol,"Interpolation, Extrapolation and Reduction of Computation Speed in Digital Filters," *IEEE Trans. on Acoustics, Speech and Signal Processing*, Vol.ASSP–22, pp.231–235, Aug.1974.

[8] R.Sudhakar, R.C.Agarwal and S.C.Dutta Roy,"Time Domain Interpolation using Differentiators," *IEEE Trans. on Acoustics, Speech and Signal Processing*, Vol.ASSP–30, pp.992–997, Dec.1982.

[9] L.R.Rabiner and B.Gold,*Theory and Application of Digital Signal Processing*, Prectice-Hall Inc., Englewood Cliffs, New Jersey, 1975, Chapter 3.

[10] J.F.Kaiser,"Nonrecursive Digital Filter Design using the I_0–sinh Window Function," *Proc. 1974 IEEE Int. Symp. Circuits Syst.*, pp.20–23, Apr.1974.

[11] L.Pelkowitz,"Frequency Domain Analysis of Wraparound Error in Fast Convolution Algorithms," *IEEE Trans. on Acoustics, Speech and Signal Processing*, Vol.ASSP–29, pp.413–422, Jun.1981.

[12] T.G.Stockham,"High Speed Convolution and Correlation," *Proc. 1966 Spring Joint Comput. Conf.*, AFIPS, Vol.28, pp.229–233, 1966.

[13] F.J.Harris,"On the Use of Windows for Harmonic Analysis with the Discrete Fourier Transform," *Proc. of the IEEE*, Vol.66, No.1, pp.51–83, Jan.1978.

[14] C.M.Loeffler and R.E.Leonard Jr.,"Phase Unwrapping via Median Filtering," *ICASSP 84 Proc.*, Vol.3, pp.46.8.1–3, Mar.1984.

[15] H.W.Bode,*Network Analysis and Feedback Amplifier Design*, D.Van Nostrand Company Inc., New York, 1945, Chapter XII, pp.305–309.

[16] A.V.Oppenheim and R.W.Schafer, *Digital Signal Processing*, Prentice-Hall Inc., Englewood Cliffs, New Jersey, 1975, Chapter 7, pp.344–350.

[17] L.R.Rabiner, B.Gold and C.A.McGonegal,"An Approach to the Approximation Problem for Nonrecursive Digital Filters," *IEEE Trans. on Acoustics, Speech and Signal Processing*, Vol.ASSP–18, pp.83–106, Jun.1970.

[18] M.E.Weber and R.Heisler,"A Frequency-Domain Beamforming Algorithm for Wideband, Coherent Signal Processing," *J. Acoust. Soc. Am.*, Vol.76, No.6, pp.1132–1144, Oct.1984.

UNCLASSIFIED

Security Classification

DOCUMENT CONTROL DATA - R & D

(Security classification of title, body of abstract and indexing annotation must be entered when the overall document is classified)

1 ORIGINATING ACTIVITY DEFENCE RESEARCH ESTABLISHMENT ATLANTIC	2a. DOCUMENT SECURITY CLASSIFICATION UNCLASSIFIED 2b. GROUP

3. DOCUMENT TITLE

NOVEL METHODS OF DIGITAL PHASE SHIFTING TO ACHIEVE ARBITRARY VALUES OF TIME DELAY

4. DESCRIPTIVE NOTES (Type of report and inclusive dates)

5. AUTHOR(S) (Last name, first name, middle initial)

MOHAMMED, A.

6. DOCUMENT DATE SEPTEMBER 1985	7a. TOTAL NO. OF PAGES 44	7b. NO. OF REFS 18
8a. PROJECT OR GRANT NO.	9a. ORIGINATOR'S DOCUMENT NUMBER(S) DREA REPORT 85/106	
8b. CONTRACT NO.	9b. OTHER DOCUMENT NO.(S) (Any other numbers that may be assigned this document)	

10. DISTRIBUTION STATEMENT

11. SUPPLEMENTARY NOTES	12. SPONSORING ACTIVITY

13. ABSTRACT

In many signal processing applications such as in underwater acoustic array beamforming, the need arises to implement digital phase shifters. Conventional methods of implementation make use of digital interpolation and decimation to derive FIR(Finite-duration Impulse Response) realizations. Such filters, however, are capable of providing delays that are only rational fractions of the unit delay. To obtain delays that are arbitrary factors of the unit delay, two novel methods are presented: the first method makes use of a windowing technique and the second method makes use of a frequency-sampling approach. In both methods the constraint of exactly linear phase is relaxed and the departures from linear phase are kept very small. To ensure that the new phase shifters attain a high level of performance, comprehensive error measures have been developed and applied; these performance measures consist of a normalized rms error, the phase delay error and the group delay error. Moreover, these error measures are applicable to any method of designing digital phase shifters. In addition, for the frequency-sampling designs, the concept of an effective filter length is introduced; this concept takes into account the wraparound error that arises in fast-convolution signal processing operations. Aside from the presentation of the design procedures and error measures, examples are included to illustrate the salient features of the two new methods.

DSIS
78-10

KEY WORDS

DIGITAL PHASE SHIFTERS
WINDOWING
FREQUENCY-SAMPLING
TIME DELAY REALIZATION
BEAMFORMING TIME DELAY

INSTRUCTIONS

1. **ORIGINATING ACTIVITY**: Enter the name and address of the organization issuing the document.

2a. **DOCUMENT SECURITY CLASSIFICATION**: Enter the overall security classification of the document including special warning terms whenever applicable.

2b. **GROUP**: Enter security reclassification group number. The three groups are defined in Appendix 'M' of the DRB Security Regulations.

3. **DOCUMENT TITLE**: Enter the complete document title in all capital letters. Titles in all cases should be unclassified. If a sufficiently descriptive title cannot be selected without classification, show title classification with the usual one-capital-letter abbreviation in parentheses immediately following the title.

4. **DESCRIPTIVE NOTES**: Enter the category of document, e.g. technical report, technical note or technical letter. If appropriate, enter the type of document, e.g. interim, progress, summary, annual or final. Give the inclusive dates when a specific reporting period is covered.

5. **AUTHOR(S)**: Enter the name(s) of author(s) as shown on or in the document. Enter last name, first name, middle initial. If military, show rank. The name of the principal author is an absolute minimum requirement.

6. **DOCUMENT DATE**: Enter the date (month, year) of Establishment approval for publication of the document.

7a. **TOTAL NUMBER OF PAGES**: The total page count should follow normal pagination procedures, i.e., enter the number of pages containing information.

7b. **NUMBER OF REFERENCES**: Enter the total number of references cited in the document.

8a **PROJECT OR GRANT NUMBER**: If appropriate, enter the applicable research and development project or grant number under which the document was written.

8b. **CONTRACT NUMBER**: If appropriate, enter the applicable number under which the document was written.

9a. **ORIGINATOR'S DOCUMENT NUMBER(S)**: Enter the official document number by which the document will be identified and controlled by the originating activity. This number must be unique to this document.

9b. **OTHER DOCUMENT NUMBER(S)**: If the document has been assigned any other document numbers (either by the originator or by the sponsor), also enter this number(s).

10. **DISTRIBUTION STATEMENT**: Enter any limitations on further dissemination of the document, other than those imposed by security classification, using standard statements such as:

    (1) "Qualified requesters may obtain copies of this document from their defence documentation center."

    (2) "Announcement and dissemination of this document is not authorized without prior approval from originating activity."

11. **SUPPLEMENTARY NOTES**: Use for additional explanatory notes.

12. **SPONSORING ACTIVITY**: Enter the name of the departmental project office or laboratory sponsoring the research and development. Include address.

13. **ABSTRACT**: Enter an abstract giving a brief and factual summary of the document, even though it may also appear elsewhere in the body of the document itself. It is highly desirable that the abstract of classified documents be unclassified. Each paragraph of the abstract shall end with an indication of the security classification of the information in the paragraph (unless the document itself is unclassified) represented as (TS), (S), (C), (R), or (U).

    The length of the abstract should be limited to 20 single-spaced standard typewritten lines; 7½ inches long.

14. **KEY WORDS**: Key words are technically meaningful terms or short phrases that characterize a document and could be helpful in cataloging the document. Key words should be selected so that no security classification is required. Identifiers, such as equipment model designation, trade name, military project code name, geographic location, may be used as key words but will be followed by an indication of technical context.

END

FILMED

1-86

DTIC